

**A New Fit Assessment Framework for Common Factor Models Using
Generalized Residuals**

Youjin Sung, Youngjin Han, and Yang Liu
University of Maryland

arXiv:2405.15204v1 [stat.ME] 24 May 2024

Author Note

Correspondence should be made to Youjin Sung at 1230B Benjamin Bldg, 3942 Campus Dr, University of Maryland, College Park, MD, 20742. Email: yjsung@umd.edu. The authors would like to thank Drs. Hongyang Zhao and Patricia Alexander from University of Maryland, College Park, for providing the empirical data.

Abstract

Standard common factor models, such as the linear normal factor model, rely on strict parametric assumptions, which require rigorous model-data fit assessment to prevent fallacious inferences. However, overall goodness-of-fit diagnostics conventionally used in factor analysis do not offer diagnostic information on where the misfit originates. In the current work, we propose a new fit assessment framework for common factor models by extending the theory of generalized residuals (Haberman & Sinharay, 2013). This framework allows for the flexible adaptation of test statistics to identify various sources of misfit. In addition, the resulting goodness-of-fit tests provide more informative diagnostics, as the evaluation is performed conditionally on latent variables. Several examples of test statistics suitable for assessing various model assumptions are presented within this framework, and their performance is evaluated by simulation studies and a real data example.

Keywords: common factor model, goodness-of-fit assessment, generalized residual

A New Fit Assessment Framework for Common Factor Models Using Generalized Residuals

1. Introduction

In the fields of education and psychology, it is often of interest to study constructs that are not directly observable. These constructs cannot be directly measured and are often formulated as latent variables (LVs). Instruments are administered to collect observable indicators associated with these LVs, which are referred to as manifest variables (MVs). The LVs can then be inferred from the collected MVs by fitting a measurement model that specifies the relationship between LVs and MVs.

A widely used LV measurement model is the common factor model (e.g., Bollen, 1989; Jöreskog, 1969; Kaplan, 2008; Kline, 2023; Lawley and Maxwell, 1971), particularly when analyzing continuous data. The common factor model requires MVs to be linearly dependent on LVs, aiming to attribute the dependencies among MVs to LVs. This model has been widely used for testing theories about the number of LVs and the pattern of MV-LV dependency (i.e., confirmatory factor analysis), or for learning these structures from data (i.e., exploratory factor analysis).

Most of the commonly used measurement models, however, rely on strong parametric assumptions. For example, in the common factor model, the conditional mean of an MV given LVs is a linear function of LVs, and the conditional variance of an MV is constant. In addition, it is often assumed that the MVs and LVs are normally distributed. These restrictive assumptions may be violated when analyzing real-world data, resulting in poor model-data fit and potentially erroneous inferences.

To prevent fallacious inferences, various goodness-of-fit (GOF) assessment tools have been developed for common factor models. A majority of existing GOF diagnostics rely on residual means, residual covariances, or deviances to reflect the discrepancies between observed data and model-based predictions. Some examples of these diagnostics include the likelihood ratio test, Root Mean Square Error of Approximation (RMSEA: Steiger and Lind, 1980), Standardized Root Mean Squared Residual (SRMR: Bentler, 1995), Comparative Fit Index (CFI: Bentler, 1990), and Tucker-Lewis Index (TLI: Tucker and Lewis, 1973).

However, these classical GOF diagnostics are not ideal for assessing specific assumption violations. Because the test statistics and indices are formulated based on residual moments or deviances, misfit from various sources may offset each other. Also, even when misfit is detected, conventional GOF diagnostics do not provide information on the source of the misfit. The lack of understanding of where the misfit originates from hinders model modification.

To address these limitations, we propose a new fit assessment framework for common factor models based on the theory of generalized residuals. The generalized residual framework is a flexible tool that allows for evaluating various model-based predictions by comparing them with corresponding observed statistics. It was originally proposed by Haberman and Sinharay (2013) and has been successfully used in item response theory (IRT) to assess specific parametric assumptions of the model (e.g., functional forms of item characteristic curves and normality of the LV; Haberman et al., 2019; Haberman et al., 2013; Monroe, 2021; van Rijn et al., 2016). A prominent feature of the generalized residuals is their asymptotically normality, which enables formal statistical tests. In addition, generalized residuals are defined conditionally on LV values, allowing for local assessments. In cases where the latent dimensionality is low (e.g., one or two), graphical displays can also be conveniently generated, providing intuitive diagnostics for assumption violations.

In the current work, we extend the theory of generalized residuals to common factor models with continuous MVs. This extension allows us to identify various sources of misfit in common factor models, such as the nonlinear relationship between MVs and LVs, heterogeneous variance of MVs conditional on LVs, and nonnormality of LVs. In addition, we suggest a summary GOF statistic that complements the local statistics conditional on LV values, which can facilitate an overall judgment on misfit. For all the proposed GOF statistics, we derive asymptotic reference distributions to construct formal statistical tests. Ultimately, our proposed framework is expected to complement conventional GOF diagnostics for common factor models.

The rest of the paper is organized as follows. In Section 2, we introduce the common factor model and present our extended theory of generalized residuals, along with example GOF test statistics suitable for testing various model assumptions. In Section 3, the performance of the proposed test statistics are evaluated by Monte Carlo studies. In Section 4, our GOF testing methods are illustrated with a real data example. The paper is concluded with a discussion of the main findings and future directions in Section 5.

2. Theory

2.1. Common Factor Model

2.1.1. Latent Variable Measurement Model

Let $Y_{ij} \in \mathcal{R}$ be the individual i 's response for manifest variable (MV) j , and $\mathbf{X}_i = (X_{i1}, \dots, X_{id})^\top \in \mathcal{R}^d$ be the d -dimensional latent variable (LV) for individual i . Denote the conditional density of $Y_{ij}|\mathbf{X}_i$ by $f_j(y_{ij}|\mathbf{x})$, where y_{ij} and $\mathbf{x} = (x_1, \dots, x_d)^\top$ indicate the realized values of Y_{ij} and \mathbf{X}_i , respectively. Let $\mathbf{Y}_i = (Y_{i1}, \dots, Y_{im})^\top$ be a

collection of m MVs from the same individual i . It is typically assumed that Y_{i1}, \dots, Y_{im} are conditionally independent given \mathbf{X}_i , often referred to as the local independence assumption (McDonald, 1999. pp. 255-257). The conditional density of $\mathbf{Y}_i = \mathbf{y}_i = (y_{i1}, \dots, y_{im})^\top$ given $\mathbf{X}_i = \mathbf{x}$ can then be factorized as

$$f(\mathbf{y}_i|\mathbf{x}) = \prod_{j=1}^m f_j(y_{ij}|\mathbf{x}). \quad (1)$$

It follows that the marginal density/likelihood of $\mathbf{Y}_i = \mathbf{y}_i$ is obtained as the following integral

$$f(\mathbf{y}_i) = \int \prod_{j=1}^m f_j(y_{ij}|\mathbf{x}) \phi(\mathbf{x}) d\mathbf{x}, \quad (2)$$

in which ϕ denotes the population density of \mathbf{X}_i .

Pooling across a sample of n independent and identically distributed (i.i.d.) random vectors of MVs, the sample log-likelihood can be expressed as

$$\ell_n(\boldsymbol{\xi}; \mathbf{Y}) = \sum_{i=1}^n \log f(\mathbf{y}_i; \boldsymbol{\xi}), \quad (3)$$

in which $\mathbf{Y} = (\mathbf{Y}_1, \dots, \mathbf{Y}_n)^\top \in \mathcal{R}^{n \times m}$ denotes the data matrix, and the dependency on model parameters, denoted as $\boldsymbol{\xi} \in \mathcal{R}^q$, is now included in the notation. In parametric LV measurement models where the distribution of LVs and the conditional distribution of MVs given LVs are specified, $\boldsymbol{\xi}$ is often estimated by maximum likelihood (ML). ML estimation seeks for $\boldsymbol{\xi}$ that solves the following estimating equation

$$\nabla_{\boldsymbol{\xi}} \ell_n(\boldsymbol{\xi}; \mathbf{Y}) = \mathbf{0}, \quad (4)$$

in which $\nabla_{\boldsymbol{\xi}} \ell_n(\boldsymbol{\xi}; \mathbf{Y})$ is a $1 \times q$ vector of partial derivatives of $\ell_n(\boldsymbol{\xi}; \mathbf{Y})$ with respect to $\boldsymbol{\xi}$. The solution to Equation 4 is denoted $\hat{\boldsymbol{\xi}}$. Under suitable regularity conditions, $\hat{\boldsymbol{\xi}}$ corresponds to a local maximum of the sample log-likelihood function.

2.1.2. Common Factor Model

In the current work, we focus on a special LV measurement model for continuous MVs; namely, the common factor model. We assume that $\mathbf{X}_i \sim \mathcal{N}(\mathbf{0}, \boldsymbol{\Phi})$ and that $Y_{ij}|\mathbf{X}_i = \mathbf{x} \sim \mathcal{N}(\nu_j + \boldsymbol{\lambda}_j^\top \mathbf{x}, \theta_j)$ for $j = 1, \dots, m$, where ν_j denotes an intercept, $\boldsymbol{\lambda}_j$ denotes a $d \times 1$ vector of factor loadings, and θ_j denotes an error variance. The conditional density

$f_j(y_{ij}|\mathbf{x})$ is expressed as

$$f_j(y_{ij}|\mathbf{x}) = \frac{1}{\sqrt{2\pi\theta_j}} \exp\left(-\frac{1}{2\theta_j}(y_j - (\nu_j + \boldsymbol{\lambda}_j^\top \mathbf{x}))^2\right). \quad (5)$$

The marginal likelihood $f(\mathbf{y}_i)$ can then be deduced from Equation 2, which amounts to a normal density function for $\mathcal{N}(\boldsymbol{\nu}, \boldsymbol{\Lambda}\boldsymbol{\Phi}\boldsymbol{\Lambda}^\top + \boldsymbol{\Theta})$:

$$f(\mathbf{y}_i) = (2\pi)^{-\frac{m}{2}} \det(\boldsymbol{\Lambda}\boldsymbol{\Phi}\boldsymbol{\Lambda}^\top + \boldsymbol{\Theta})^{-\frac{1}{2}} \exp\left(-\frac{1}{2}(\mathbf{y}_i - \boldsymbol{\nu})^\top (\boldsymbol{\Lambda}\boldsymbol{\Phi}\boldsymbol{\Lambda}^\top + \boldsymbol{\Theta})^{-1}(\mathbf{y}_i - \boldsymbol{\nu})\right), \quad (6)$$

in which $\boldsymbol{\nu}$ is a $m \times 1$ vector of intercepts, $\boldsymbol{\Lambda}$ is a $m \times d$ matrix of factor loadings, and $\boldsymbol{\Theta}$ is an $m \times m$ diagonal matrix with elements $\theta_1, \dots, \theta_m$. The model parameters $\boldsymbol{\xi}$ now consist of free elements in $\boldsymbol{\nu}$, $\boldsymbol{\Lambda}$, $\boldsymbol{\Phi}$, and $\boldsymbol{\Theta}$, and $\hat{\boldsymbol{\xi}}$ can be obtained by solving Equation 4 with a normal log-likelihood $\ell_n(\boldsymbol{\xi}; \mathbf{Y})$.

2.2. Empirical Estimators for Conditional Expectations

In this section, we start with defining the population conditional expectation of interest under the common factor model and present two empirical estimators of it, which will be used to construct generalized residuals.

First, let $\eta(\mathbf{x}, \boldsymbol{\xi})$ be the conditional expectation of a function $h(\mathbf{x}, \mathbf{Y}_i, \boldsymbol{\xi})$ such that

$$\eta(\mathbf{x}, \boldsymbol{\xi}) = \mathbb{E}[h(\mathbf{x}, \mathbf{Y}_i, \boldsymbol{\xi})|\mathbf{x}] = \int h(\mathbf{x}, \mathbf{y}_i, \boldsymbol{\xi}) f(\mathbf{y}_i|\mathbf{x}) d\mathbf{y}_i. \quad (7)$$

In Equation 7, the function h is allowed to depend on the LVs \mathbf{x} , the MVs \mathbf{y}_i , and the model parameters $\boldsymbol{\xi}$. Using the Bayes theorem, η can be alternatively expressed as

$$\eta(\mathbf{x}, \boldsymbol{\xi}) = \frac{1}{\phi(\mathbf{x})} \int h(\mathbf{x}, \mathbf{y}_i, \boldsymbol{\xi}) \frac{f(\mathbf{y}_i|\mathbf{x})\phi(\mathbf{x})}{f(\mathbf{y}_i)} f(\mathbf{y}_i) d\mathbf{y}_i = \frac{1}{\phi(\mathbf{x})} \mathbb{E}[h(\mathbf{x}, \mathbf{Y}_i, \boldsymbol{\xi}) f(\mathbf{x}|\mathbf{Y}_i)]. \quad (8)$$

Equation 8 is more favorable for the purpose of constructing empirical estimators because the population expectation on the right-hand side can be conveniently estimated by a sample average. Assuming an i.i.d. sample $\mathbf{Y}_1, \dots, \mathbf{Y}_n$, two types of estimators for η can be constructed, which are henceforth termed the simple estimator and the ratio estimator, respectively.

2.2.1. Simple Estimator

Replacing the population expectation on the right-hand side of Equation 8 with the sample mean yields the simple estimator

$$\hat{\eta}(\mathbf{x}, \boldsymbol{\xi}) = \frac{1}{\phi(\mathbf{x})} \frac{1}{n} \sum_{i=1}^n h(\mathbf{x}, \mathbf{Y}_i, \boldsymbol{\xi}) f(\mathbf{x}|\mathbf{Y}_i) = \frac{1}{n} \sum_{i=1}^n \frac{h(\mathbf{x}, \mathbf{Y}_i, \boldsymbol{\xi}) f(\mathbf{Y}_i|\mathbf{x})}{f(\mathbf{Y}_i)}. \quad (9)$$

Let

$$H(\mathbf{x}, \mathbf{Y}_i, \boldsymbol{\xi}) = \frac{h(\mathbf{x}, \mathbf{Y}_i, \boldsymbol{\xi})f(\mathbf{Y}_i|\mathbf{x})}{f(\mathbf{Y}_i)} \quad (10)$$

be a shorthand notation for the summand on the right-hand side of Equation 9. Then η and $\hat{\eta}$ can be expressed more concisely as follows:

$$\hat{\eta}(\mathbf{x}, \boldsymbol{\xi}) = \frac{1}{n} \sum_{i=1}^n H(\mathbf{x}, \mathbf{Y}_i, \boldsymbol{\xi}), \quad (11)$$

$$\eta(\mathbf{x}, \boldsymbol{\xi}) = \mathbb{E}[H(\mathbf{x}, \mathbf{Y}_i, \boldsymbol{\xi})]. \quad (12)$$

When the model is correctly specified with known parameters, the Central Limit Theorem (CLT; Bickel and Doksum, 2015, p. 470) implies that

$$\sqrt{n}[\hat{\eta}(\mathbf{x}, \boldsymbol{\xi}) - \eta(\mathbf{x}, \boldsymbol{\xi})] \xrightarrow{d} \mathcal{N}(0, \sigma_H^2(\mathbf{x}, \boldsymbol{\xi})), \quad (13)$$

in which $\sigma_H^2(\mathbf{x}, \boldsymbol{\xi}) = \text{Var}[H(\mathbf{x}, \mathbf{Y}_i, \boldsymbol{\xi})]$.

2.2.2. Ratio Estimator

An alternative estimator, which we call the ratio estimator, is defined as

$$\tilde{\eta}(\mathbf{x}, \boldsymbol{\xi}) = \frac{\frac{1}{n} \sum_{i=1}^n h(\mathbf{x}, \mathbf{Y}_i, \boldsymbol{\xi})f(\mathbf{x}|\mathbf{Y}_i)}{\frac{1}{n} \sum_{i=1}^n f(\mathbf{x}|\mathbf{Y}_i)}. \quad (14)$$

The ratio estimator can be alternatively conceived as the ratio of two simple estimators $\hat{\eta}_n$ and $\hat{\eta}_d$, where $\hat{\eta}_n$ is given by Equation 9 (or Equation 11) and $\hat{\eta}_d$ is an empirical estimator of 1, obtained by setting $h = 1$ in Equation 9. In other words, the ratio estimator is equivalently expressed as

$$\tilde{\eta}(\mathbf{x}, \boldsymbol{\xi}) = \frac{\hat{\eta}_n(\mathbf{x}, \boldsymbol{\xi})}{\hat{\eta}_d(\mathbf{x}, \boldsymbol{\xi})} = \frac{\frac{1}{n} \sum_{i=1}^n H_n(\mathbf{x}, \mathbf{Y}_i, \boldsymbol{\xi})}{\frac{1}{n} \sum_{i=1}^n H_d(\mathbf{x}, \mathbf{Y}_i, \boldsymbol{\xi})}, \quad (15)$$

in which we let $H_n(\mathbf{x}, \mathbf{Y}_i, \boldsymbol{\xi})$ and $H_d(\mathbf{x}, \mathbf{Y}_i, \boldsymbol{\xi})$ denote the summands of the numerator and denominator respectively:

$$H_n(\mathbf{x}, \mathbf{Y}_i, \boldsymbol{\xi}) = \frac{h(\mathbf{x}, \mathbf{Y}_i, \boldsymbol{\xi})f(\mathbf{Y}_i|\mathbf{x})}{f(\mathbf{Y}_i)}, \quad (16)$$

$$H_d(\mathbf{x}, \mathbf{Y}_i, \boldsymbol{\xi}) = \frac{f(\mathbf{Y}_i|\mathbf{x})}{f(\mathbf{Y}_i)}. \quad (17)$$

By the CLT again, the sample mean of Equations 16 and 17 are jointly asymptotically normal. It then follows from the Delta method that

$$\begin{aligned} & \sqrt{n} \left[\frac{\hat{\eta}_n(\mathbf{x}, \boldsymbol{\xi})}{\hat{\eta}_d(\mathbf{x}, \boldsymbol{\xi})} - \frac{\eta_n(\mathbf{x}, \boldsymbol{\xi})}{\eta_d(\mathbf{x}, \boldsymbol{\xi})} \right] \\ & \xrightarrow{d} \mathcal{N} \left(0, \frac{\sigma_{H_n}^2(\mathbf{x}, \boldsymbol{\xi})}{\eta_d^2(\mathbf{x}, \boldsymbol{\xi})} - 2 \frac{\eta_n(\mathbf{x}, \boldsymbol{\xi})}{\eta_d^3(\mathbf{x}, \boldsymbol{\xi})} \sigma_{H_n H_d}(\mathbf{x}, \boldsymbol{\xi}) + \frac{\eta_n^2(\mathbf{x}, \boldsymbol{\xi})}{\eta_d^4(\mathbf{x}, \boldsymbol{\xi})} \sigma_{H_d}^2(\mathbf{x}, \boldsymbol{\xi}) \right), \end{aligned} \quad (18)$$

in which $\sigma_{H_n}^2(\mathbf{x}, \boldsymbol{\xi}) = \text{Var}[H_n(\mathbf{x}, \mathbf{Y}_i, \boldsymbol{\xi})]$, $\sigma_{H_d}^2(\mathbf{x}, \boldsymbol{\xi}) = \text{Var}[H_d(\mathbf{x}, \mathbf{Y}_i, \boldsymbol{\xi})]$, and $\sigma_{H_n H_d}(\mathbf{x}, \boldsymbol{\xi}) = \text{Cov}[H_n(\mathbf{x}, \mathbf{Y}_i, \boldsymbol{\xi}), H_d(\mathbf{x}, \mathbf{Y}_i, \boldsymbol{\xi})]$.

2.2.3. Examples: Choices of h

In both simple and ratio estimators, the choice of the function $h(\mathbf{x}, \mathbf{Y}_i, \boldsymbol{\xi})$ is crucial as it determines the population conditional expectations we aim to estimate from our data. Here, we present three examples.

One choice for h is $h(\mathbf{x}, \mathbf{Y}_i, \boldsymbol{\xi}) = \phi(\mathbf{x})$, which leads to the estimator for the LV density, $\phi(\mathbf{x})$, by

$$\hat{\eta}(\mathbf{x}, \boldsymbol{\xi}) = \frac{1}{n} \sum_{i=1}^n \frac{\phi(\mathbf{x}) f(\mathbf{Y}_i | \mathbf{x})}{f(\mathbf{Y}_i)}, \quad (19)$$

$$\eta(\mathbf{x}, \boldsymbol{\xi}) = \mathbb{E} \left(\frac{1}{n} \sum_{i=1}^n \frac{\phi(\mathbf{x}) f(\mathbf{Y}_i | \mathbf{x})}{f(\mathbf{Y}_i)} \right) = \phi(\mathbf{x}). \quad (20)$$

By the Bayes formula, $\frac{\phi(\mathbf{x}) f(\mathbf{Y}_i | \mathbf{x})}{f(\mathbf{Y}_i)} = f(\mathbf{x} | \mathbf{Y}_i)$, the right-hand side of Equation 19 becomes the sample average of $f(\mathbf{x} | \mathbf{Y}_i)$, which is the posterior density of \mathbf{x} given \mathbf{Y}_i . This form of estimator has been used in the context of IRT (Monroe, 2021) to detect misfit in the LV density under unidimensional IRT models.

Another example is $h(\mathbf{x}, \mathbf{Y}_i, \boldsymbol{\xi}) = Y_{ij}$, which yields an empirical estimator of $\mathbb{E}(Y_{ij} | \mathbf{x})$, the conditional expectation of an MV given the LVs. In the case of a unidimensional IRT model with dichotomous response variables, this choice of h reduces to the empirical estimator for item characteristic curves (e.g., Haberman et al., 2013) which has been used for item-level fit assessments of the IRT model by comparing it with the model-implied counterparts. With the common factor model, $\mathbb{E}(Y_{ij} | \mathbf{x})$ becomes a linear function in \mathbf{x} . Therefore, the simple or ratio estimators using this function h can be used to assess the linearity assumption at the MV level.

Similarly, the idea can be extended to fit assessments involving higher-order conditional moments. For instance, setting $h(\mathbf{x}, \mathbf{Y}_i, \boldsymbol{\xi}) = [Y_{ij} - \mathbb{E}(Y_{ij} | \mathbf{x})]^2$ leads to an empirical estimator of $\text{Var}(Y_{ij} | \mathbf{x})$, which is assumed to be constant across \mathbf{x} under the common factor model. Such an MV-level homoscedasticity assumption can be assessed by

residuals defined by this h .

Regarding the choice between the simple and ratio estimators, the simple estimator is the only viable option for the first example. This is because the ratio estimator $\tilde{\eta}(\mathbf{x}, \boldsymbol{\xi})$ simplifies to $\phi(\mathbf{x})$, which is no longer random. On the other hand, the second and third examples are compatible with both estimators, allowing us to choose between them. We recommend using the ratio estimator in those cases because the ratio estimator directly estimates the LV density, whereas the simple estimator relies on the correct specification of the LV density by its formula. In cases when the LV density is misspecified, the simple estimator will respond not only to the sources of misfit of interest but also to the misspecified LV density, leading to less specific fit diagnostics compared to the ratio estimator. Further discussion on this will be provided in the supplementary document using a real data example.

2.3. Residuals

When the model holds and all model parameters are assumed to be known, both simple and ratio estimators converge to $\eta(\mathbf{x}, \boldsymbol{\xi})$, the population conditional expectation of interest implied by the model. The discrepancy of $\hat{\eta}(\mathbf{x}, \hat{\boldsymbol{\xi}})$ or $\tilde{\eta}(\mathbf{x}, \hat{\boldsymbol{\xi}})$ from $\eta(\mathbf{x}, \boldsymbol{\xi})$ therefore reflects disagreement between data and the model. In practice, however, model parameters need to be estimated from the data. Taking this qualification into account, we define residuals (pointwise in \mathbf{x}) as

$$e_S(\mathbf{x}) = \hat{\eta}(\mathbf{x}, \hat{\boldsymbol{\xi}}) - \eta(\mathbf{x}, \hat{\boldsymbol{\xi}}) \quad (21)$$

$$e_R(\mathbf{x}) = \tilde{\eta}(\mathbf{x}, \hat{\boldsymbol{\xi}}) - \eta(\mathbf{x}, \hat{\boldsymbol{\xi}}), \quad (22)$$

in which the subscripts S and R represent the simple and ratio estimators, respectively, and $\hat{\boldsymbol{\xi}}$ is the ML estimator that satisfies

$$\sqrt{n}(\hat{\boldsymbol{\xi}} - \boldsymbol{\xi}) \xrightarrow{d} \mathcal{N}(\mathbf{0}, \mathcal{I}^{-1}(\boldsymbol{\xi})) \quad (23)$$

under the correctly specified model as $n \rightarrow \infty$. $\mathcal{I}(\boldsymbol{\xi}) = \mathbb{E} \left[\nabla_{\boldsymbol{\xi}} \log f(\mathbf{Y}_i; \boldsymbol{\xi})^\top \nabla_{\boldsymbol{\xi}} \log f(\mathbf{Y}_i; \boldsymbol{\xi}) \right]$ denotes the $q \times q$ per-observation Fisher information matrix.

Our goal now is to analyze the asymptotic behavior of these residuals so that we can obtain formal statistical tests on various types of misfit. To achieve this goal, we present an extended theory of generalized residuals in Sections 2.3.1. and 2.3.2., which establishes the asymptotic multivariate normality of residuals in a context more general than Haberman and Sinharay (2013). We further propose quadratic form statistic in Section 2.3.3. that summarizes pointwise results and derive its asymptotic reference distribution. In Section 2.3.4., a brief discussion is given on estimating the asymptotic

covariance matrices (ACMs) of residuals. Finally, in Section 2.3.5., specific test statistics are derived using the three examples provided in Section 2.2.3.

2.3.1. Asymptotic Normality of Residuals

Consider a $k \times 1$ residual vector, $\mathbf{e} \in \mathcal{R}^k$, expressed as

$$\mathbf{e}(\mathbf{X}) = \hat{\boldsymbol{\eta}}(\mathbf{X}, \hat{\boldsymbol{\xi}}) - \boldsymbol{\eta}(\mathbf{X}, \hat{\boldsymbol{\xi}}), \quad (24)$$

in which $\mathbf{X} = (\mathbf{x}_1, \dots, \mathbf{x}_k)^\top \in \mathcal{R}^{k \times d}$ indicates k sets of arbitrarily chosen LV vectors. In Equation 24, $\hat{\boldsymbol{\eta}}(\mathbf{X}, \hat{\boldsymbol{\xi}})$ and $\boldsymbol{\eta}(\mathbf{X}, \hat{\boldsymbol{\xi}})$ are defined similarly as in Section 2.2.1. as

$$\hat{\boldsymbol{\eta}}(\mathbf{X}, \hat{\boldsymbol{\xi}}) = \frac{1}{n} \sum_{i=1}^n \mathbf{H}(\mathbf{X}, \mathbf{Y}_i, \hat{\boldsymbol{\xi}}), \quad (25)$$

$$\boldsymbol{\eta}(\mathbf{X}, \hat{\boldsymbol{\xi}}) = \mathbb{E}[\mathbf{H}(\mathbf{X}, \mathbf{Y}_i, \hat{\boldsymbol{\xi}})], \quad (26)$$

in which

$$\mathbf{H}(\mathbf{X}, \mathbf{Y}_i, \hat{\boldsymbol{\xi}}) = (H_1(\mathbf{x}_1, \mathbf{Y}_i, \hat{\boldsymbol{\xi}}), H_2(\mathbf{x}_2, \mathbf{Y}_i, \hat{\boldsymbol{\xi}}), \dots, H_k(\mathbf{x}_k, \mathbf{Y}_i, \hat{\boldsymbol{\xi}}))^\top, \quad (27)$$

is a $k \times 1$ vector. Each component in the right-hand side vector in Equation 27 is formed by different choices of the function h and/or by different LV values. In the supplementary document, we establish the following asymptotic normality result for these residuals

$$\sqrt{n}\mathbf{e}(\mathbf{X}) \xrightarrow{d} \mathcal{N}(\mathbf{0}, -\mathbf{A}(\mathbf{X}, \boldsymbol{\xi})\mathcal{I}^{-1}(\boldsymbol{\xi})\mathbf{A}(\mathbf{X}, \boldsymbol{\xi})^\top + \boldsymbol{\Sigma}_{\mathbf{H}}(\mathbf{X}, \boldsymbol{\xi})), \quad (28)$$

in which $\mathbf{A}(\mathbf{X}, \boldsymbol{\xi}) = \mathbb{E}[\mathbf{H}(\mathbf{X}, \mathbf{Y}_i, \boldsymbol{\xi})\nabla_{\boldsymbol{\xi}} \log f(\mathbf{Y}_i; \boldsymbol{\xi})]$ and $\boldsymbol{\Sigma}_{\mathbf{H}}(\mathbf{X}, \boldsymbol{\xi}) = \text{Cov}[\mathbf{H}(\mathbf{X}, \mathbf{Y}_i, \boldsymbol{\xi})]$.

As a special case, if we consider using a fixed type of function h but Q different evaluation points of LV values to construct \mathbf{H} , we get

$$\mathbf{H}(\mathbf{X}, \mathbf{Y}_i, \hat{\boldsymbol{\xi}}) = (H(\mathbf{x}_1, \mathbf{Y}_i, \hat{\boldsymbol{\xi}}), H(\mathbf{x}_2, \mathbf{Y}_i, \hat{\boldsymbol{\xi}}), \dots, H(\mathbf{x}_Q, \mathbf{Y}_i, \hat{\boldsymbol{\xi}}))^\top, \quad (29)$$

in which $k = Q$ with $\mathbf{X} = (\mathbf{x}_1, \dots, \mathbf{x}_Q)^\top$ and $H_1 = \dots = H_Q = H$. The corresponding residuals obtained by Equation 29 is denoted \mathbf{e}_S , a vector of residuals for the simple estimator on Q evaluation points.

2.3.2. Transformations

Let $\boldsymbol{\varphi} : \mathcal{R}^k \rightarrow \mathcal{R}^{k'}$ be a twice continuously differentiable transformation function that is simultaneously applied to $\hat{\boldsymbol{\eta}}$ and $\boldsymbol{\eta}$. Then, we can construct a $k' \times 1$ vector of transformed residuals

$$\mathbf{e}_{\boldsymbol{\varphi}}(\mathbf{X}) = \boldsymbol{\varphi}(\hat{\boldsymbol{\eta}}(\mathbf{X}, \hat{\boldsymbol{\xi}})) - \boldsymbol{\varphi}(\boldsymbol{\eta}(\mathbf{X}, \hat{\boldsymbol{\xi}})). \quad (30)$$

In the supplementary document, we establish the following asymptotic normality of the transformed residuals

$$\sqrt{n}\mathbf{e}_\varphi(\mathbf{X}) \xrightarrow{d} \mathcal{N}(\mathbf{0}, \nabla\varphi(\boldsymbol{\eta}(\mathbf{X}, \boldsymbol{\xi}))(-\mathbf{A}(\mathbf{X}, \boldsymbol{\xi})\boldsymbol{\mathcal{I}}^{-1}(\boldsymbol{\xi})\mathbf{A}(\mathbf{X}, \boldsymbol{\xi})^\top + \boldsymbol{\Sigma}_{\mathbf{H}}(\mathbf{X}, \boldsymbol{\xi}))\nabla\varphi(\boldsymbol{\eta}(\mathbf{X}, \boldsymbol{\xi}))^\top), \quad (31)$$

in which $\nabla\varphi$ stands for a $k' \times k$ Jacobian matrix of φ .

The residual for the ratio estimator is subsumed as a special case of the transformed residual with an appropriate choice of \mathbf{H} and φ . To obtain the ratio estimator, first, formulate a $2Q \times 1$ vector \mathbf{H} as follows

$$\mathbf{H}(\mathbf{X}, \mathbf{Y}_i, \hat{\boldsymbol{\xi}}) = (H_n(\mathbf{x}_1, \mathbf{Y}_i, \hat{\boldsymbol{\xi}}), \dots, H_n(\mathbf{x}_Q, \mathbf{Y}_i, \hat{\boldsymbol{\xi}}), H_d(\mathbf{x}_1, \mathbf{Y}_i, \hat{\boldsymbol{\xi}}), \dots, H_d(\mathbf{x}_Q, \mathbf{Y}_i, \hat{\boldsymbol{\xi}}))^\top, \quad (32)$$

in which H_n and H_d have been defined in Equations 16 and 17. With this formulation in Equation 32, we have $k = 2Q$ with $\mathbf{X} = (\mathbf{x}_1, \dots, \mathbf{x}_Q, \mathbf{x}_1, \dots, \mathbf{x}_Q)^\top$, $H_1 = \dots = H_Q = H_n$ and $H_{Q+1} = \dots = H_{2Q} = H_d$. Second, obtain the corresponding $\hat{\boldsymbol{\eta}}$ and $\boldsymbol{\eta}$ as in Equations 25 and 26. Then, applying a transformation function $\varphi : \mathcal{R}^{2Q} \rightarrow \mathcal{R}^Q$,

$$\varphi(\boldsymbol{\gamma}) = \left(\frac{\gamma_1}{\gamma_{Q+1}}, \dots, \frac{\gamma_Q}{\gamma_{2Q}} \right)^\top \quad (33)$$

with $\boldsymbol{\gamma} = (\gamma_1, \dots, \gamma_Q, \gamma_{Q+1}, \dots, \gamma_{2Q})^\top$ to $\hat{\boldsymbol{\eta}}$ and $\boldsymbol{\eta}$ provides a vector of ratio estimator residuals on $k' = Q$ evaluation points, which we denote by \mathbf{e}_R .

2.3.3. Summary Statistics

Let $\mathbf{e}_\varphi(\mathbf{X})$ denote transformed residuals at Q different evaluation points (i.e., $k' = Q$) and $\boldsymbol{\Sigma}_\varphi$ denote the ACM of \mathbf{e}_φ :

$$\boldsymbol{\Sigma}_\varphi(\mathbf{X}, \boldsymbol{\xi}) = \nabla\varphi(\boldsymbol{\eta}(\mathbf{X}, \boldsymbol{\xi}))(-\mathbf{A}(\mathbf{X}, \boldsymbol{\xi})\boldsymbol{\mathcal{I}}^{-1}(\boldsymbol{\xi})\mathbf{A}(\mathbf{X}, \boldsymbol{\xi})^\top + \boldsymbol{\Sigma}_{\mathbf{H}}(\mathbf{X}, \boldsymbol{\xi}))\nabla\varphi(\boldsymbol{\eta}(\mathbf{X}, \boldsymbol{\xi}))^\top. \quad (34)$$

Based on the joint asymptotic normality result in Equation 31, a quadratic form statistic can be constructed using \mathbf{e}_φ as follows:

$$T = n\mathbf{e}_\varphi^\top \mathbf{W} \mathbf{e}_\varphi, \quad (35)$$

in which \mathbf{W} is a $Q \times Q$ symmetric matrix. Once the asymptotic distribution is derived, this quadratic form statistic can be used to summarize pointwise results across multiple evaluation points of LVs.

When the model is correctly specified, it is known that T is asymptotically distributed as a mixture of independent χ_1^2 random variables by the general theory of quadratic form statistics with normal random variables (Box, 1954). The correct p -value

for this mixture of χ^2 distribution can be computed, for example, by the inversion formula given in Imhof (1961) or by adjusting T by its mean and variance, approximating a χ^2 distribution (Satorra and Bentler, 1994; Satterthwaite, 1946). However, p -value calculation under a χ^2 -mixture reference can often be complicated.

To simplify the calculation of p -values, we consider a weight matrix \mathbf{W} such that the resulting T is asymptotically χ^2 . In particular, it is known that when

$$\Sigma_\varphi \mathbf{W} \Sigma_\varphi \mathbf{W} \Sigma_\varphi = \Sigma_\varphi \mathbf{W} \Sigma_\varphi \quad (36)$$

is satisfied and $\text{tr}(\mathbf{W} \Sigma_\varphi) = s$, T is asymptotically distributed as a χ^2 distribution with s degrees of freedom (e.g., Schott, 2016, Theorem 11.11). One way to satisfy these conditions is by defining the weight matrix as the Moore-Penrose pseudoinverse Σ_φ^+ (Magnus and Neudecker, 1999, p. 36) of Σ_φ . This approach has been used to construct quadratic form fit statistics in previous studies (e.g., Liu and Maydeu-Olivares, 2014; Liu et al., 2019; Reiser, 1996). However, some drawbacks of using Σ_φ^+ as the weight matrix have also been pointed out (Maydeu-Olivares & Joe, 2008). To summarize, the rank of Σ_φ needs to be estimated by the number of non-zero eigenvalues for a sample estimate of Σ_φ , where this non-zero counting depends on arbitrary tolerance we set for zero eigenvalues, making the approach numerically unstable.

To overcome some of the difficulties, we propose defining the weight matrix as

$$\mathbf{W} = \Sigma_\varphi^- = \mathbf{U} \mathbf{\Omega}^- \mathbf{U}^\top. \quad (37)$$

In Equation 37, the $Q \times Q$ matrix \mathbf{U} contains the Q eigenvectors of Σ_φ (i.e., $\Sigma_\varphi = \mathbf{U} \mathbf{\Omega} \mathbf{U}^\top$ by the eigendecomposition where $\mathbf{\Omega}$ is the diagonal matrix of eigenvalues), and $\mathbf{\Omega}^- = \text{diag}(\omega_1^{-1}, \dots, \omega_s^{-1}, 0, \dots, 0)$. $\mathbf{\Omega}^-$ stands for the inverse of $\mathbf{\Omega}$ only with the s ($s \leq \text{rank}(\Sigma_\varphi)$) largest eigenvalues, $\omega_1, \dots, \omega_s$. Σ_φ^- is a generalized inverse of Σ_φ , such that $\Sigma_\varphi^- \Sigma_\varphi \Sigma_\varphi^- = \Sigma_\varphi^-$ holds. In the case where $s = \text{rank}(\Sigma_\varphi)$, Σ_φ^- reduces to the pseudoinverse Σ_φ^+ . With this formulation, Equation 36 and $\text{tr}(\Sigma_\varphi^- \Sigma_\varphi) = s$ are met, and we obtain the following limiting reference distribution

$$n \mathbf{e}_\varphi^\top \Sigma_\varphi^- \mathbf{e}_\varphi \xrightarrow{d} \chi_s^2. \quad (38)$$

Now, given that Equation 38 holds as long as $1 \leq s \leq \text{rank}(\Sigma_\varphi)$, a sufficiently small number for s , such as $s = 1$, can be chosen as the reference degrees of freedom. This way, the numerical issues involved with using Σ_φ^+ as the weight matrix can be avoided. The performance of our proposed approach with the choice of $s = 1$ will be evaluated in our simulation studies in Section 3.

In this section, we present the summary statistic only for the transformed residuals because the residuals without transformation (i.e., \mathbf{e} in Section 2.3.1.) are a special case of \mathbf{e}_φ with the identity transformation. The quadratic form in Equation 35 subsumes $n\mathbf{e}^\top \mathbf{W}\mathbf{e}$ as a special case, so the asymptotic result in Equation 38 also applies to \mathbf{e} .

2.3.4. Estimation of the Asymptotic Covariance Matrix

In applications, the ACMs of residuals (Equations 28 and 31) need to be estimated from the data. When the population ACM is substituted with its consistent estimator, the asymptotic normality results remain unchanged by the Slutsky's theorem (Bickel and Doksum, 2015, p. 512).

To obtain the consistent estimators of the ACMs in Equations 28 and 31, we replace $\boldsymbol{\xi}$ with the ML estimator $\hat{\boldsymbol{\xi}}$ wherever they appear in the formula. For estimating the population mean and (co)variance in $\mathbf{A}(\mathbf{X}, \hat{\boldsymbol{\xi}})$ and $\boldsymbol{\Sigma}_{\mathbf{H}}(\mathbf{X}, \hat{\boldsymbol{\xi}})$, one simplest way is to compute the sample mean and sample covariance matrix, which has been adopted by Haberman et al. (2013) and Monroe (2021). However, our pilot simulation study revealed that this approach leads to severely inflated Type I error rates with extreme LV values, particularly when the sample size is small. Therefore, we suggest to obtain more stable estimates for $\mathbf{A}(\mathbf{X}, \hat{\boldsymbol{\xi}})$ and $\boldsymbol{\Sigma}_{\mathbf{H}}(\mathbf{X}, \hat{\boldsymbol{\xi}})$ by computing the Monte Carlo (MC) mean and covariance as follows:

1. Sample $\tilde{\mathbf{y}}_i, i = 1, \dots, M$, from the marginal distribution of \mathbf{Y}_i with density $f(\mathbf{y}_i; \hat{\boldsymbol{\xi}})$.
2. Use $\tilde{\mathbf{y}}_i$ to calculate $\mathbf{H}(\mathbf{x}, \tilde{\mathbf{y}}_i, \hat{\boldsymbol{\xi}})$ and $\nabla_{\boldsymbol{\xi}} \log f(\tilde{\mathbf{y}}_i; \hat{\boldsymbol{\xi}})$.
3. Estimate $\mathbf{A}(\mathbf{X}, \hat{\boldsymbol{\xi}})$ and $\boldsymbol{\Sigma}_{\mathbf{H}}(\mathbf{X}, \hat{\boldsymbol{\xi}})$ by

$$\hat{\mathbf{A}}(\mathbf{X}, \hat{\boldsymbol{\xi}}) = \frac{1}{M} \sum_{i=1}^M \left[\mathbf{H}(\mathbf{x}, \tilde{\mathbf{y}}_i, \hat{\boldsymbol{\xi}}) \nabla_{\boldsymbol{\xi}} \log f(\tilde{\mathbf{y}}_i; \hat{\boldsymbol{\xi}}) \right], \quad (39)$$

$$\hat{\boldsymbol{\Sigma}}_{\mathbf{H}}(\mathbf{X}, \hat{\boldsymbol{\xi}}) = \frac{1}{M-1} \sum_{i=1}^M \left[\left(\mathbf{H}(\mathbf{x}, \tilde{\mathbf{y}}_i, \hat{\boldsymbol{\xi}}) - \bar{\mathbf{H}}(\mathbf{x}, \tilde{\mathbf{y}}_i, \hat{\boldsymbol{\xi}}) \right) \left(\mathbf{H}(\mathbf{x}, \tilde{\mathbf{y}}_i, \hat{\boldsymbol{\xi}}) - \bar{\mathbf{H}}(\mathbf{x}, \tilde{\mathbf{y}}_i, \hat{\boldsymbol{\xi}}) \right)^\top \right]. \quad (40)$$

In Equation 40, $\bar{\mathbf{H}}(\mathbf{x}, \tilde{\mathbf{y}}_i, \hat{\boldsymbol{\xi}}) = \frac{1}{M} \sum_{i=1}^M \mathbf{H}(\mathbf{x}, \tilde{\mathbf{y}}_i, \hat{\boldsymbol{\xi}})$. By the law of large numbers and Slutsky's theorem, $\hat{\mathbf{A}}(\mathbf{X}, \hat{\boldsymbol{\xi}}) \xrightarrow{p} \mathbf{A}(\mathbf{X}, \boldsymbol{\xi})$ and $\hat{\boldsymbol{\Sigma}}_{\mathbf{H}}(\mathbf{X}, \hat{\boldsymbol{\xi}}) \xrightarrow{p} \boldsymbol{\Sigma}_{\mathbf{H}}(\mathbf{X}, \boldsymbol{\xi})$.

In the subsequent notation for ACMs, a caret “^” is added to indicate that the ACMs are obtained using $\hat{\boldsymbol{\xi}}$, $\hat{\mathbf{A}}$, and $\hat{\boldsymbol{\Sigma}}_{\mathbf{H}}$.

2.3.5. Examples: Test Statistics

Based on the theory presented in previous sections, two types of formal statistical tests are developed to provide evidence for model misfit: 1) a large-sample z -test at fixed LV values; 2) a large sample χ^2 -test summarizing misfit across multiple LV grids.

In light of Equation 31, let $e_{\varphi,r}(\mathbf{x}_r)$ be the r th component of \mathbf{e}_{φ} evaluated at \mathbf{x}_r and $\hat{\sigma}_{\varphi,r}$ be the square-root of the r th diagonal entry of $\hat{\Sigma}_{\varphi}$. Then, the standardized residual can be defined pointwise as

$$z(\mathbf{x}_r) = \frac{e_{\varphi,r}(\mathbf{x}_r)}{SE[e_{\varphi,r}(\mathbf{x}_r)]}, \quad r = 1, \dots, Q, \quad (41)$$

in which the standard error (SE) estimate for $e_{\varphi,r}(\mathbf{x}_r)$ is denoted by $SE[e_{\varphi,r}(\mathbf{x}_r)] = \hat{\sigma}_{\varphi,r}(\mathbf{x}_r)/\sqrt{n}$. Equation 41 converges in distribution to $\mathcal{N}(0, 1)$ under the null hypothesis that the model is correctly specified. The values of $|z(\mathbf{x}_r)|$ larger than 1.96 suggest significant misfit at $\alpha = 0.05$. In addition, a χ^2 test statistic is constructed from Equation 38 with Σ_{φ}^{-} estimated by $\hat{\Sigma}_{\varphi}^{-}$ as

$$T = n\mathbf{e}_{\varphi}^{\top} \hat{\Sigma}_{\varphi}^{-} \mathbf{e}_{\varphi}, \quad (42)$$

which provides a summary result on multiple evaluation points. With the choice of $s = 1$, the reference distribution becomes a χ^2 distribution with 1 degree of freedom, and $T > 3.84$ suggests significant overall misfit at $\alpha = 0.05$.

Now, by varying the function h , we can obtain statistical tests suitable for evaluating various model assumptions. Using the three examples discussed in Section 2.2.3., we construct pointwise statistics, denoted by $z_1(\mathbf{x})$, $z_2(\mathbf{x})$, and $z_3(\mathbf{x})$, and summary statistics, denoted by T_1 , T_2 and T_3 , for each example, optimized for testing the assumption of LV density, MV-level linearity of the mean function, and MV-level homoscedasticity of the variance function, respectively. Table 1 provides summary information for the three examples discussed so far.

Sources of misfit	LV density	MV-level linearity	MV-level homoscedasticity
Choice for $h(\mathbf{x}, \mathbf{Y}_i, \boldsymbol{\xi})$	$\phi(\mathbf{x})$	Y_{ij}	$[Y_{ij} - \mathbb{E}(Y_{ij} \mathbf{x})]^2$
Empirical estimator	Simple	Ratio	Ratio
Pointwise statistic for z -test	$z_1(\mathbf{x})$	$z_2(\mathbf{x})$	$z_3(\mathbf{x})$
Summary statistic for χ^2 -test	T_1	T_2	T_3

Table 1

Pointwise and summary statistics for three examples discussed in Section 2.2.3.

3. Simulation Study

Two simulation studies are reported in this section. Study 1 (Section 3.1.) is for evaluating the performance of $z_1(\mathbf{x})$ and T_1 . Study 2 (Section 3.2.) is for evaluating the performance of $z_2(\mathbf{x})$, $z_3(\mathbf{x})$, T_1 , and T_2 . Within each study, we manipulate two factors: (1) sample sizes ($n = 100, 500$, and $1,000$) and (2) the presence or absence of model misspecification. Sample sizes were selected to represent small, moderate, and large samples, respectively. Empirical rejection rates are evaluated with 500 replications.

For each simulation study, we first describe the simulation setup, including the simulation conditions and data-generating models, followed by detailed procedures to calculate the test statistics (Sections 3.1.1. and 3.2.1.). We then examine the performance of them using the empirical rejection rates as evaluation criteria (Sections 3.1.2. and 3.2.2.). All computations were conducted in R (R Core Team, 2024).

3.1. Simulation Study 1

3.1.1. Simulation Setup

As a special case of the common factor model presented in Section 2.1.2., we considered a bifactor model (Holzinger & Swineford, 1937) with three dimensional LVs: one general factor (g) and two specific factors (s_1 and s_2). The number of MVs was set to ten (i.e., $m = 10$), with the first five MVs loaded on g and s_1 , and the remaining five on g and s_2 . All three LVs were assumed to be orthogonal.

For data generation, two different LV densities were specified to represent correctly specified and misspecified conditions. For the correctly specified condition, $\mathbf{X}_i, i = 1, \dots, n$ were generated from a multivariate standard normal distribution. For the misspecified condition, the following mixture of two multivariate normal distributions was used, $\mathbf{X}_i \sim 0.5\mathcal{N}(\boldsymbol{\mu}^{(1)}, \boldsymbol{\Phi}^{(1)}) + 0.5\mathcal{N}(\boldsymbol{\mu}^{(2)}, \boldsymbol{\Phi}^{(2)})$, in which $\boldsymbol{\mu}^{(1)} = (-0.8, -0.8, -0.8)^\top$, $\boldsymbol{\mu}^{(2)} = (0.8, 0.8, 0.8)^\top$, and $\boldsymbol{\Phi}^{(1)} = \boldsymbol{\Phi}^{(2)} = \text{diag}(0.6^2, 0.6^2, 0.6^2)$. Figure 1 depicts the shape of the two data-generating LV densities with respect to a marginal unidimensional LV.

For both correctly and incorrectly specified conditions, we set other data-generating parameters equally as $\boldsymbol{\nu} = \mathbf{0}$,

$$\boldsymbol{\Lambda} = \begin{bmatrix} \sqrt{0.15} & \sqrt{0.25} & \sqrt{0.35} & \sqrt{0.15} & \sqrt{0.25} & \sqrt{0.49} & \sqrt{0.21} & \sqrt{0.35} & \sqrt{0.49} & \sqrt{0.21} \\ \sqrt{0.15} & \sqrt{0.25} & \sqrt{0.35} & \sqrt{0.15} & \sqrt{0.25} & 0 & 0 & 0 & 0 & 0 \\ 0 & 0 & 0 & 0 & 0 & \sqrt{0.21} & \sqrt{0.09} & \sqrt{0.15} & \sqrt{0.21} & \sqrt{0.09} \end{bmatrix}^\top, \quad (43)$$

and $\theta_j = 1 - \boldsymbol{\lambda}_j^\top \boldsymbol{\lambda}_j, j = 1, \dots, 10$. By setting the model parameters this way, the communality for each MV alternates among 0.3, 0.5 and 0.7 in both conditions. Within each communality value, the contribution of the general factor and specific factor is made

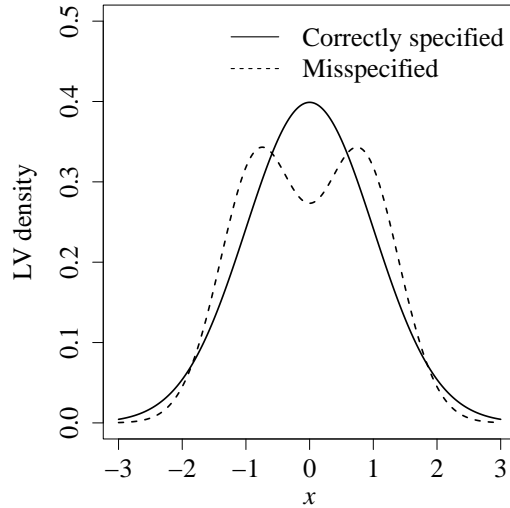


Figure 1

Data-generating LV densities for correctly specified and misspecified conditions, presented with respect to a marginal unidimensional LV.

equal for the first five MVs, while the ratio of the contribution becomes 7 to 3 for the last five MVs.

Upon generating data using the specified parameter values, the proposed tests for assessing the LV density fit were conducted using the following procedures: (1) construct the simple estimator with $h = \phi(\mathbf{x})$, (2) estimate model parameters, (3) obtain \mathbf{e}_S and its ACM, (4) compute $z_1(\mathbf{x})$ and T_1 to conduct pointwise z -tests and the overall χ^2 -test.

For parameter estimation in step 2, the lavaan package (Rosseel, 2012) was used with the default option of ML estimation with normal likelihood. Mean structure was added to the model (meanstructure = TRUE). To check model convergence, we used the following criteria: (1) the absence of Heywood cases, (2) the maximum absolute element of the gradient vector is less than 10^{-4} , and (3) the minimum eigenvalue of the Hessian matrix is greater than zero. Default maximum number of iterations was adopted. In step 3, the estimated ACM was obtained following the process described in Section 2.3.4. with $M = 10,000$. The inverse of the expected information matrix was obtained using the inverted.information option in the lavInspect function, and the gradient of the individual log-likelihood, $\nabla_{\xi} \log f(\mathbf{Y}_i; \hat{\xi})$, within the formula **A** (Equation 28) was obtained from the lavScores function. In step 4, 13 evenly spaced values between -3 to 3 were used as evaluation points per LV, resulting in a total of $13^3 = 2,197$ evaluation points for $z_1(\mathbf{x})$. For T_1 , a subgrid of $5^3 = 125$ points, obtained by 5 equally spaced values from -2 to 2 per LV, was used as an illustration. In addition, we set the degree of freedom $s = 1$ in Equation 38 so that the reference limiting distribution for T_1 becomes χ_1^2 .

As noted in existing literature (Eid et al., 2018), bifactor models tend to exhibit poor convergence, a pattern observed in our simulation study as well. For the correctly specified condition, the convergence rates were 0.43, 0.68, and 0.69 for sample sizes of 100, 500, and 1,000, respectively, rounded to two digits. For the misspecified condition, the rounded convergence rates were 0.40, 0.57, and 0.60 for each sample size condition. Given the imperfect convergence, we calculated the empirical rejection rates based only on the converged cases; namely, the empirical Type I error rate and power were computed as the ratio of rejected cases to the number of converged cases under correctly specified and misspecified condition, respectively.

3.1.2. Results

Empirical Type I error rates were investigated under the correctly specified condition at the nominal level of $\alpha = 0.05$. If the proposed tests perform well, the Type I error results should closely match the nominal level. Figure 2 illustrates the Type I error results for the pointwise z -tests (presented as points connected by lines) and the overall χ^2 -tests (presented as numbers in parentheses alongside the sample sizes) under various sample size conditions. Due to the three-dimensional nature of the LVs, it is challenging to present the results simultaneously for all LVs. Therefore, in Figure 2, we present the results separately for each LV: g , s_1 , and s_2 . Each point in the figure represents the Type I error rate evaluated at the LV value on the x -axis conditioned on the mean of the other two LVs. The results were summarized this way to avoid the influence of LV combinations that are extremely unlikely to occur, such as $\mathbf{x} = (-3, -3, 3)^\top$. In addition, 95% normal-approximation confidence intervals were obtained around the nominal α -level, which indicate an acceptable range of Type I error rates considering Monte Carlo error. Because the actual number of iterations was different for each simulation condition due to varying convergence rates, the obtained interval was slightly different for each condition. In Figure 2, we delineated the narrowest interval using the sample size condition of $n = 1,000$.

The results indicate that Type I error rates for both pointwise and overall tests are well-controlled across all sample size conditions. For the pointwise results, most of the points in Figure 2 fall within the Monte Carlo confidence interval, suggesting decent performance of $z_1(\mathbf{x})$. Some deviations are observed in the middle range of s_1 for the $n = 100$ condition; however, using the appropriate Monte Carlo confidence interval for the $n = 100$ case covers those deviations inside the interval. Other than that, a couple of points fall outside the confidence interval at extreme LV values. However, those extreme LV values have a low chance of occurrence in practice given the normal density, and the extent of their deviation from the interval was also minimal. For the summary results, the Type I error rates closely aligned with the nominal level across all sample size conditions, verifying

satisfactory performance of T_1 .

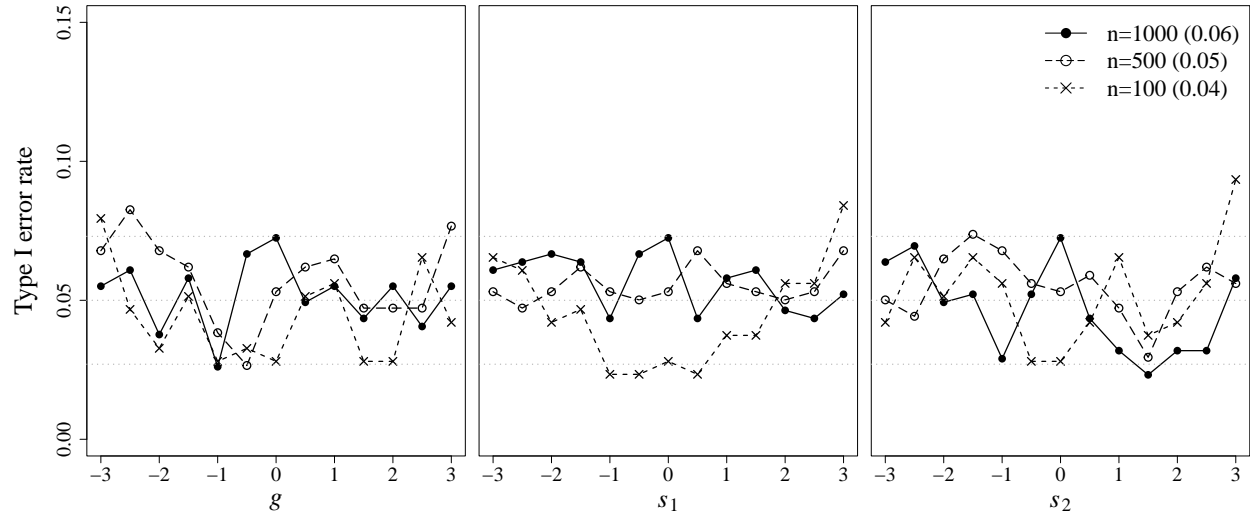


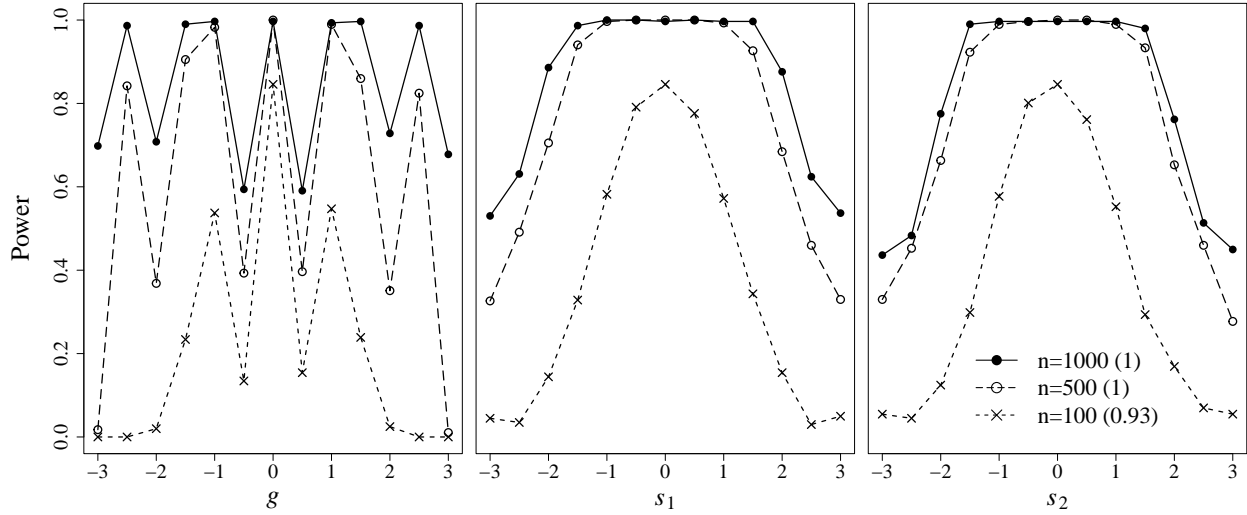
Figure 2

Type I error results for the pointwise and overall LV density fit tests at $\alpha = 0.05$. Grey-scaled horizontal dotted lines represent the nominal level $\alpha = 0.05$ and the Monte Carlo confidence interval for $n = 1,000$ condition (i.e., the narrowest interval). Pointwise z -test results are summarized for each LV—one for each column. Points in each column indicate results on the corresponding LV values conditioned on the means of the other two LVs. Overall χ^2 -test results are presented within parentheses next to the sample size legend.

Empirical power was investigated next under the misspecified condition. Figure 3 displays the power results for the pointwise z -tests and the overall χ^2 -tests under various sample size conditions. The results are summarized in the same way as in Figure 2: one column for each LV, with each point representing the power evaluated at the LV value on the x -axis conditioned on the mean of the other two LVs. Power results for the χ^2 -tests are presented in parentheses alongside the sample sizes.

In general, both pointwise and overall tests showed good power in detecting misfit. Pointwise results showed power as high as around 0.8 even with the smallest sample size condition, with further increases as sample size increased. Summary results exhibited even higher power, exceeding 0.9 across all sample size conditions.

The power results for the pointwise z -tests need more careful examination because they are dependent on the shape of the data-generating LV densities. When conducting z -tests, the simple estimator aims to recover the LV density of the misspecified condition (see Figure 1), while the model-implied estimator mimics the standard normal density. The values of $z_1(\mathbf{x})$ are obtained based on the discrepancy between these two estimators; therefore, the power is expected to be high in regions with large discrepancies and relatively low near crossover grids. In our simulation study, the general factor responded to

**Figure 3**

Power results for the pointwise and overall LV density fit tests at $\alpha = 0.05$. Pointwise z -test results are summarized for each LV—one for each column. Points in each column indicate results on the corresponding LV values conditioned on the means of the other two LVs. Overall χ^2 -test results are presented within parentheses next to the sample size legend.

this discrepancy, as can be seen by the oscillating pattern in the first column of Figure 3. However, such an oscillating pattern was not observed for the two specific factors. Instead, the power tends to be high in the middle range of the factors, whereas it decreases towards the ends. This lack of nuanced capture can be attributed to the small number of MVs loaded, even weakly, on specific factors. Given that the empirical estimator is a sample average of the posterior LV density, it is conjectured that the effect of the prior density governed the posterior of the specific factors, leading the empirical estimator to produce an LV density shape closer to the normal density than the bimodal shape that it is supposed to recover.

3.2. Simulation Study 2

3.2.1. Simulation Setup

In Study 2, the linear normal one-factor model with $X_i \sim \mathcal{N}(0, 1)$ was under investigation with or without the misspecification in MV-level mean/variance functions. Introduce the notation μ_j and σ_j^2 for the mean and variance of the conditional distribution $Y_{ij}|X_i$. Under the linear normal factor model, $Y_{ij}|X_i = x \sim \mathcal{N}(\mu_j(x), \sigma_j^2(x))$ with the mean function $\mu_j(x) = \nu_j + \lambda_j x$ and variance function $\sigma_j^2(x) = \theta_j$. MV-level fit assessments were performed by investigating the linearity of μ_j and homoscedasticity of σ_j^2 .

The data-generating model consists of four types of MVs summarized in Table 2. The four types were determined by fully crossing linear vs. quadratic mean functions and

constant vs. log-linear variance functions, labeled as LMCV, QMCV, LMLV, and QMLV, respectively. Regardless of the type of MVs, the intercept was set to zero, i.e., $\nu_j = 0$, and the error variance was obtained by $\theta_j = 1 - \lambda_j^2$. The factor loading λ_j was set to alternate between $\sqrt{0.3}$, $\sqrt{0.5}$, and $\sqrt{0.7}$ for LMCVs; λ_j was fixed at $\sqrt{0.5}$ for the other three types of MVs. After that, coefficients κ_j , γ_{0j} , and γ_{1j} were added for the misspecified MVs. The quadratic coefficient κ_j for QMCV and QMLV was fixed at -0.1 ; γ_{0j} and γ_{1j} for LMLV and QMLV were set as $\gamma_{0j} = \log \theta_j$ and $\gamma_{1j} = 0.3$, respectively. Figure 4 illustrates the shape of $\mu_j(x)$ and $\sigma_j(x)$ with and without these additional coefficients, the combination of which comprises four types of MVs. As an illustration, $\nu_j = 0$, $\lambda_j = \sqrt{0.5}$, and $\theta_j = 0.5$ were used for this figure.

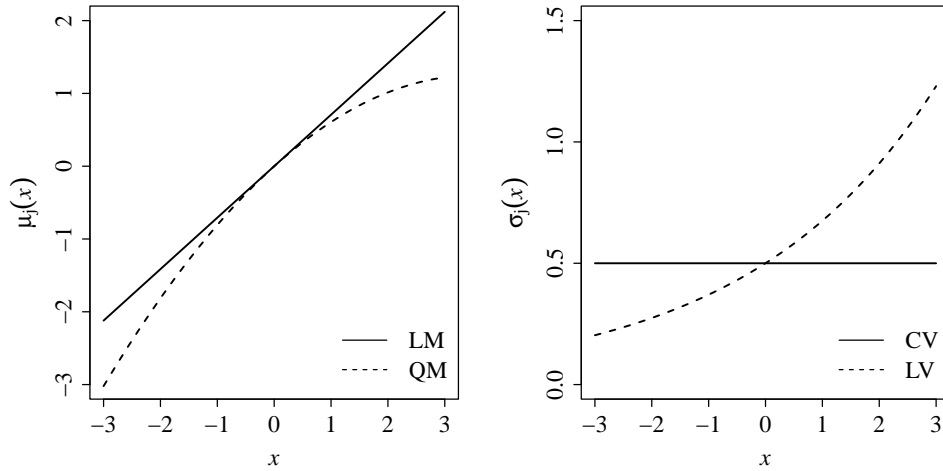
Type	Label	Conditional distribution	Misspecification
1	LMCV	$\mathcal{N}(\nu_j + \lambda_j x, \theta_j)$	Correctly specified
2	QMCV	$\mathcal{N}(\nu_j + \lambda_j x + \kappa_j x^2, \theta_j)$	Misspecified mean
3	LMLV	$\mathcal{N}(\nu_j + \lambda_j x, \exp(\gamma_{0j} + \gamma_{1j} x))$	Misspecified variance
4	QMLV	$\mathcal{N}(\nu_j + \lambda_j x + \kappa_j x^2, \exp(\gamma_{0j} + \gamma_{1j} x))$	Misspecified mean and variance

Table 2

Four types of MVs used for data generation. LMCV: linear mean function, constant variance function. QMCV: quadratic mean function, constant variance function. LMLV: linear mean function, log-linear variance function. QMLV: quadratic mean function, log-linear variance function.

For both correctly and incorrectly specified conditions, the number of MVs was fixed to ten ($m = 10$). Among the ten MVs, all of them were LMCVs in the correctly specified condition, whereas three misspecified MVs—one for LMLV, QMCV, and QMLV, respectively—were included in the misspecified condition. The first seven MVs in the misspecified condition were set to be correct in order to evaluate the empirical false detection rate—the proportion of which the tests falsely detect the correctly specified MVs as misfitting MVs in the presence of both correctly and incorrectly specified MVs.

Upon generating the data, the proposed MV-level fit assessments were performed using the following procedures: (1) construct ratio estimators with $h = Y_{ij}$ and $h = [Y_{ij} - \mathbb{E}(Y_{ij}|x)]^2$, (2) estimate model parameters, (3) obtain \mathbf{e}_R and its ACM for each estimator, (4) compute $z_2(x)$, $z_3(x)$, T_2 , and T_3 to conduct pointwise z -tests and the overall χ^2 -test. Computational details follow Study 1 as have been introduced in Section 3.1.1. except for the number of evaluation points used. In step 4, we adopted 31 evenly spaced LV values between -3 and 3 as evaluation points for $z_2(x)$ and $z_3(x)$. Among these, 11 sub-points ranging from -2 and 2 were chosen to construct T_2 and T_3 . No convergence

**Figure 4**

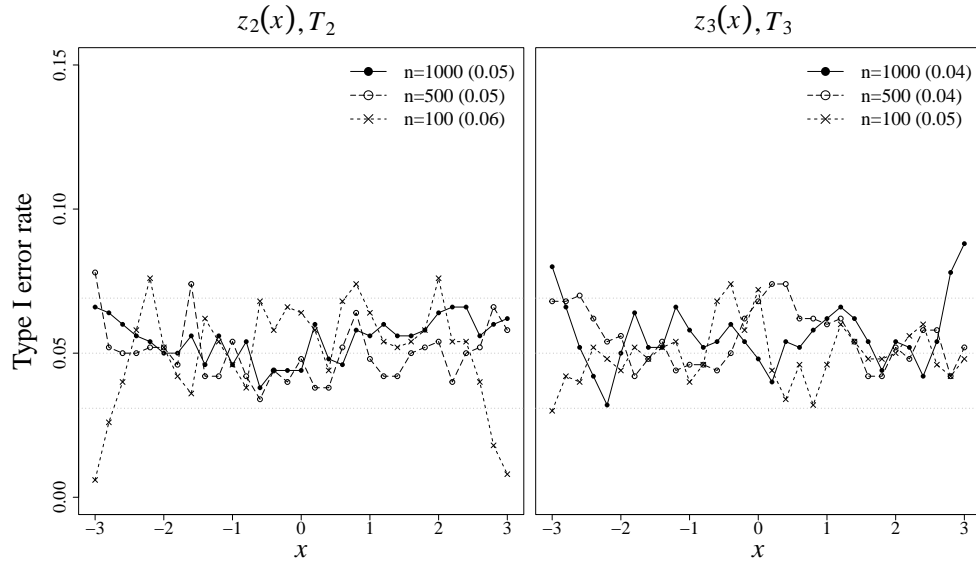
The left panel illustrates the mean function, $\mu_j(x)$, for correctly specified and misspecified conditions in the data-generating model. The right panel shows the variance function, $\sigma_j(x)$, for both conditions. LM: linear mean, QM: quadratic mean, CV: constant variance, LV: log-linear variance.

issues were found for these one-factor models; thus, the empirical rejection rates were calculated as the ratio of the rejected cases among the 500 replications.

3.2.2. Results

Empirical Type I error rates were investigated under the correctly specified condition at the nominal level of $\alpha = 0.05$. Figure 5 illustrates the Type I error results for the pointwise z -tests (presented as points connected by lines) and the overall χ^2 -tests (presented as numbers in parentheses alongside the sample sizes) under various sample size conditions. The performance of $z_2(x)$ and T_2 , which assess the linearity of μ_j , is presented in the left panel, while the performance of $z_3(x)$ and T_3 , which assess the homoscedasticity of σ_j , is presented in the right panel. In the figure, 95% normal-approximation confidence intervals are delineated around the nominal α -level, indicating an acceptable range of Type I error rates considering Monte Carlo error. Results for only one MV ($j = 2$ with communality 0.5) are presented due to space limit, but similar results were found for the other nine MVs in the correctly specified condition.

The results demonstrate that Type I error rates are well-controlled for both pointwise and overall tests across all sample size conditions. In the pointwise results, the majority of points in Figure 5 fall within the Monte Carlo confidence interval, suggesting decent performance of $z_2(x)$ and $z_3(x)$. Some noticeable deviations are observed in the extreme range of the LV; however, these extreme LV values close to -3 and 3 under the standard normal density have a rare chance of occurrence in practice, making them of no

**Figure 5**

Type I error results for the pointwise and overall MV-level fit tests at $\alpha = 0.05$. The left panel shows the results for $z_2(x)$ and T_2 ; the right panel shows the results for $z_3(x)$ and T_3 . Grey-scaled horizontal dotted lines represent the nominal level $\alpha = 0.05$ and the Monte Carlo confidence interval. Pointwise z -test results are evaluated at 31 equally spaced LV values from -3 to 3 and connected with lines. Overall χ^2 -test results are presented within parentheses next to the sample size legends. The results are presented for one MV ($j = 2$) in the correctly specified condition. Similar results were observed for the other MVs.

significant concern. Overall χ^2 -test results closely match with the nominal level across all sample size conditions, verifying the satisfactory performance of T_2 and T_3 .

Next, empirical power was investigated under the misspecified condition, and the results are summarized in Figure 6. The first row of the graphical table presents results for $z_2(x)$ and T_2 , and the second row shows results for $z_3(x)$ and T_3 . Each column contains results for QMCV, LMLV, and QMLV, respectively.

The proposed MV-level fit tests exhibited distinct behaviors in terms of power depending on the types of MVs. Specifically, $z_2(x)$ and T_2 show decent power only against QMCV and QMLV, indicating that they are mainly responsive to detecting misspecification in μ_j but not in σ_j . On the other hand, $z_3(x)$ and T_3 show decent power only against LMLV and QMLV, demonstrating the opposite pattern. These results suggest that the two types of statistics, developed respectively for testing μ_j and σ_j , perform their intended roles effectively. However, with the small sample of $n = 100$, the power tends to be low for all statistics, with little differentiation observed in their respective roles.

Another notable observation is the oscillating pattern of the power for z -tests, which is again related to the data-generating μ_j and σ_j illustrated in Figure 4. For both μ_j and

σ_j , the power is expected to be low in the middle and high towards the ends of the LV range. The performance of $z_3(x)$ demonstrated the expected pattern within approximately the 95% range of the LV. However, for $z_2(x)$, the power was unexpectedly high in the middle range of the LV. Further investigation revealed that this behavior is due to the estimation of the mean structure. With the mean structure included in the model, the LM and QM lines in Figure 4 no longer intersect at one point but at two points when QM is pulled up above LM, leading to the discrepancy captured by $z_2(x)$ and thus to high power in the middle.

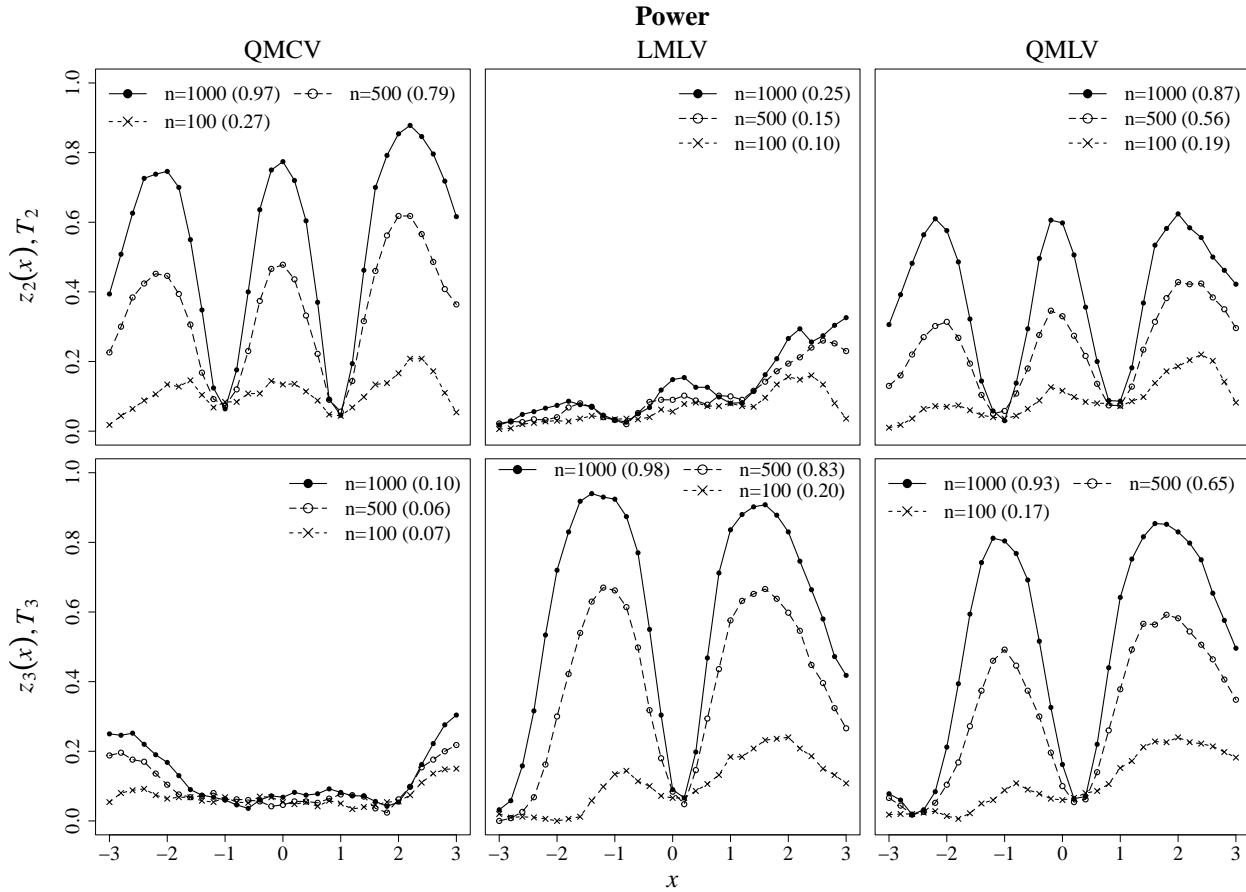


Figure 6

Power results for the pointwise and overall MV-level fit tests. The first row of the figure shows the results for $z_2(x)$ and T_2 ; the second row shows the results for $z_3(x)$ and T_3 . Each column represents results for QMCV, LMLV, and QMLV (i.e., $j = 8, 9$, and 10 in the misspecified condition). Pointwise z -test results are evaluated at 31 equally spaced LV values from -3 to 3 and connected with lines. Overall χ^2 -test results are presented within parentheses next to the sample size legends.

Finally, empirical false detection rates were examined using correctly specified MVs

(i.e., LMCVs) in the misspecified condition. The results are presented in Figure 7, in which the performance of $z_2(x)$ and T_2 is presented in the left panel, while the performance of $z_3(x)$ and T_3 is presented in the right panel. Again, we provide results for only one MV ($j = 2$ with communality 0.5); similar results were observed for the other six LMCVs in the misspecified condition.

In the presence of misspecified MVs in a model, every correctly specified MV will eventually be detected as misfit with a large enough sample size. Hence, the extent to which the rate of false detection is controlled at a low level is another crucial evaluation criterion for MV-level fit tests. In our simulation, false detection rates for both pointwise and overall statistics were well-controlled without substantial inflation, indicating their capability of distinguishing between good-fitting and bad-fitting MVs. The rates were similar to the nominal α -level in the middle range of the LV. Some inflation was observed in the extreme high end of the LV with the large sample sizes ($n = 500$ and/or 1000); however, these LV values close to 3 are again have a rare chance of occurrence in reality.

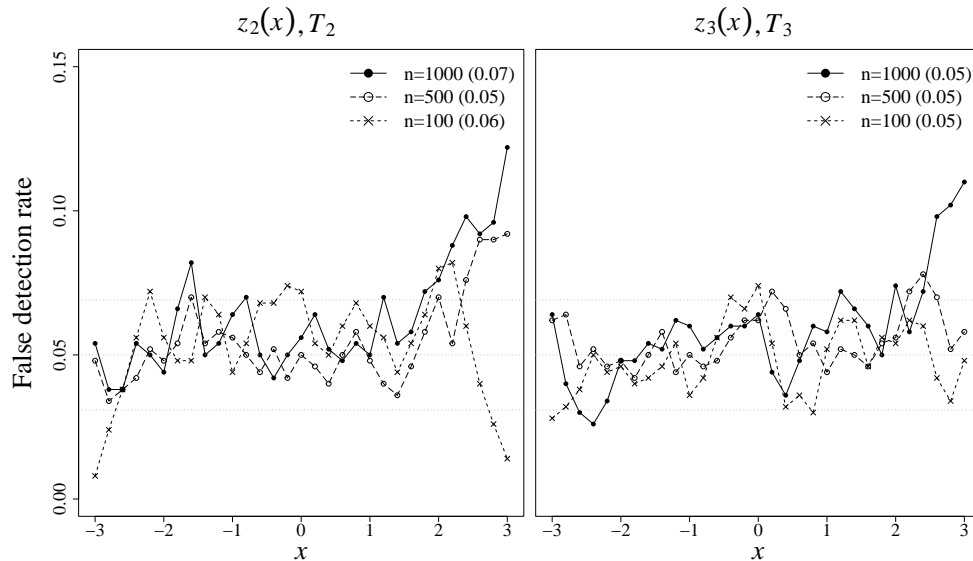


Figure 7

False detection rates for the pointwise and overall MV-level fit tests at $\alpha = 0.05$. The left panel shows the result for $z_2(x)$ and T_2 ; the right panel shows the results for $z_3(x)$ and T_3 . Grey-scaled horizontal dotted lines represent the nominal level $\alpha = 0.05$ and the Monte Carlo confidence interval. Pointwise z -test results are evaluated at 31 equally spaced LV values from -3 to 3 and connected with lines. Overall χ^2 -test results are presented within parentheses next to the sample size legends. The results are presented for one LMCV ($j = 2$) in the misspecified condition. Similar results were observed for the other six LMCVs.

4. Empirical Example

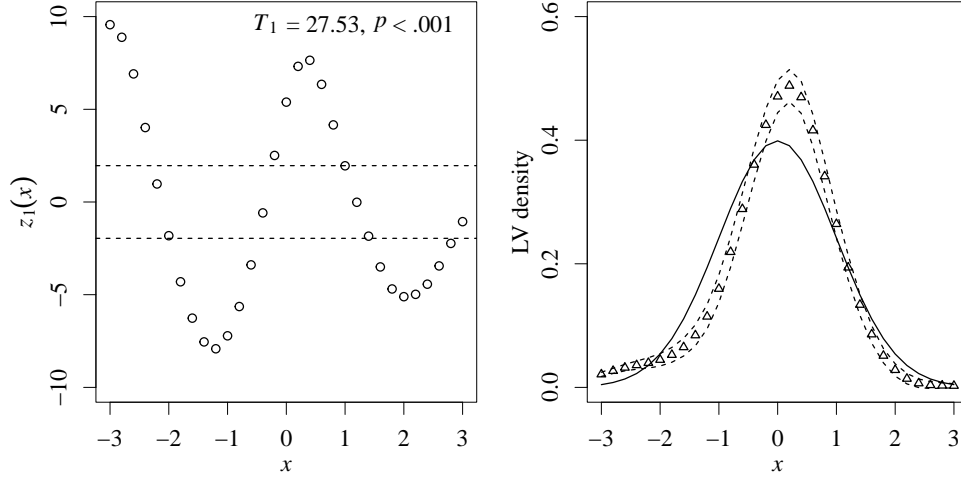
In this section, we apply the proposed fit assessment method to analyze item-level response time (RT) data, obtained from an online administration of the Test of Relational Reasoning-Junior (TORRjr) among Chinese elementary and middle school students (Zhao et al., 2021). Among the four subscales of TORRjr, we focus on the antinomy subscale, which consists of eight dichotomously scored, multiple-choice items ($m = 8$). The analyzed sample comprises $n = 744$ observations with no missing data. The same RT data were analyzed by Liu and Wang (2022) using a semiparametric approach. Additional information about TORRjr can be found, for example, in Alexander et al. (2016).

In the RT literature, van der Linden’s log-normal RT model (van der Linden, 2006) stands out as one of the most widely used models. This model is essentially the same as the linear normal one-factor model fitted to the log-transformed RT. Consequently, in our subsequent analyses, we log-transform the RT data for each item and fit the linear normal one-factor model. The LV x in this context is interpreted as latent slowness, where higher values of x indicate slower responses. When fitting the model to this log-RT data, traditional goodness-of-fit diagnostics suggest a decent fit. For example, CFI=0.98, TLI=0.97, SRMR=0.02, and RMSEA=0.06, all falling within the acceptable range according to rules of thumb presented by Hu and Bentler (1999). Although the χ^2 model fit test result indicates a poor fit of the model at $\alpha = 0.05$ ($\chi^2_{20} = 71.89, p = 0$), the test result is often ignored due to the tendency of the χ^2 test to suggest a bad fit with large sample sizes.

4.1. Fit Diagnostics

Here, we apply our proposed test statistics to evaluate the normality of the LV density, as well as the item-level linearity and homoscedasticity, all of which are fundamental assumptions in the linear normal factor model. In each analysis described below, we use 31 equally spaced LV values as evaluation points, and all of them are used to summarize the results (i.e., to obtain T_1, T_2 , and T_3). Other specific options are applied identically to those used in the simulation studies presented in the previous sections.

Figure 8 presents the results for the LV density fit tests, in which two versions of diagnostics are provided. In the left panel, the standardized residuals $z_1(x)$ are displayed as circled points, with T_1 and p -value for the χ^2 -test presented at the top. Horizontal dashed lines are drawn at ± 1.96 , representing a 95% pointwise confidence band under $\alpha = 0.05$. The right panel delivers the same information but shows results using model-implied (solid line) and empirical (triangular points) estimators. For the LV density fit test, we used the simple estimator, making the discrepancy between the two estimators at each point $e_s(x)$. Dashed lines indicate a 95% pointwise confidence band constructed by

**Figure 8**

LV density fit test results at $\alpha = 0.05$. The left panel displays results with respect to test statistics, $z_1(x)$ and T_1 . The right panel contains the same information as the left panel, but results are presented in term of model-implied (solid line) and empirical (triangular points) estimators. Dashed-lines indicate a 95% pointwise confidence band.

$$\hat{\eta}(x, \hat{\xi}) \pm 1.96[SE(e_S(x))] \text{ (see Equation 41).}$$

As observed in both panels, it is evident that the normality assumption of the LV density is violated in this example. Pointwise analyses reveal that the density is leptokurtic as well as slightly negatively skewed. This finding mirrors descriptive statistics reported in Table 2 of Liu and Wang (2022), which showed that the marginal log-RT distributions were leptokurtic and/or skewed for some items. The overall test using T_1 also exhibited substantial misfit in LV density ($T_1 = 27.53, p < .001$).

Next, item-level fit was evaluated by examining the mean and variance functions of log-RT. Figures 9 and 10 display the results for the mean function and variance function, respectively, using the model-implied (solid lines) and empirical (triangular points) estimators. For item fit analyses, we used the ratio estimator, consistent with the approach in the simulation study; thus, the discrepancy between the two estimators becomes $e_R(x)$ at each point. Dotted lines in each panel represent a 95% pointwise confidence band computed by $\tilde{\eta}(x, \hat{\xi}) \pm 1.96SE[e_R(x)]$ (see Equation 41). The p -values for the overall χ^2 test using T_2 or T_3 are provided at the top for each item.

Upon examining the pointwise results in Figure 9, it is apparent that items 2, 6, and 7 exhibit a greater number of misfitting points and a larger degree of misfit compared to the other five items, suggesting potential curvature in the mean function of those items. In particular, items 2 and 7 exhibit approximately a quadratic shape within the $[-2.5, 2.5]$ range of the LV. The summary results are consistent with the pointwise inspection,

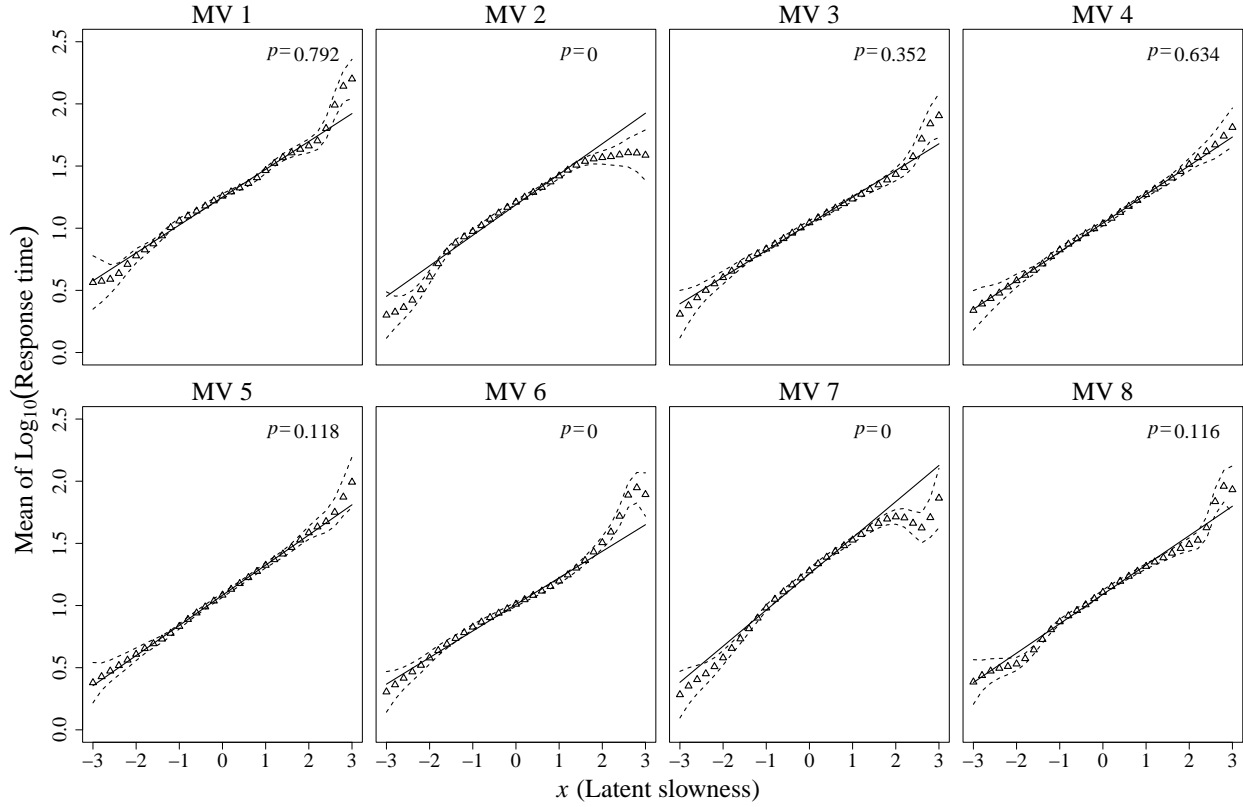


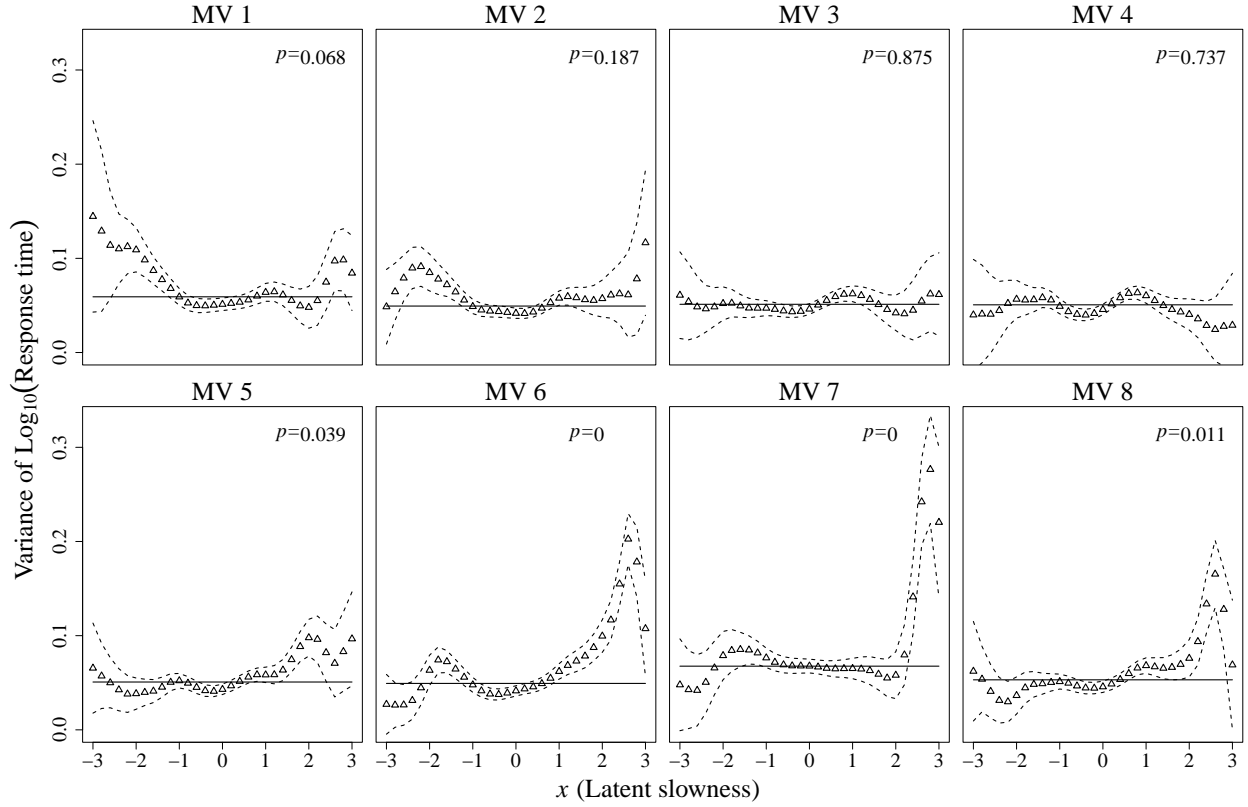
Figure 9

Empirical and model-implied mean functions for the log-transformed RT. Solid lines represent model-implied linear mean functions. Triangular points are the ratio estimators obtained at each point. Dashed lines delineate a 95% pointwise confidence band. p stands for the p -value of the overall χ^2 -test using T_2 .

detecting items 2, 6, and 7 as misfitting items. Regarding the variance function in Figure 10, most items deviate noticeably from the confidence bands, except for items 3 and 4. The deviations indicate the heteroscedastic variance depending on the level of the latent processing speed. Particularly, item 6 exhibits clear violations of the assumption across approximately 95% middle range of the LV. Item 7, on the other hand, shows decent fit across most of the LV range, with substantial misfit only in the extreme high end of the LV. Pooling all pointwise results, summary statistics detected items 5, 6, 7, and 8 as misfitting items.

5. Discussion

Based on our extended theory of generalized residuals, we propose asymptotically normal and χ^2 statistics to identify misfit in the LV density and MV-level conditional moments. Results from two simulation studies indicate that the proposed tests have well-controlled Type I error rate even with small sample sizes and decent power to detect

**Figure 10**

Empirical and model-implied variance functions for the log-transformed RT. Solid lines represent model-implied constant variance functions. Triangular points are the ratio estimators obtained at each point. Dashed lines delineate a 95% pointwise confidence band. p stands for the p -value of the overall χ^2 -test using T_3 .

misfit with moderate to large sample sizes. We conclude from these simulation results that generalized residuals are useful tools for assessing parametric assumptions involved in common factor models.

Results from the empirical example further illustrates the practical utility of our approach. In contrast to the conventional GOF diagnostics that suggested an overall decent fit of the linear normal one-factor model, our method detected misfit in various model assumptions: misfit in the LV density, the MV-level mean function, and the MV-level variance function.

In factor analysis, it is common to assume the joint multivariate normality of MVs and LVs in order to perform ML estimation. Various well-known methods exist for assessing normality at the level of observed variables (e.g., Mardia, 1970; Mardia, 1980); however, to our knowledge, assessing the normality assumption for LVs is less common. This LV-level misfit can be conveniently assessed by generalized residuals, which sometimes

can explain non-normality at the MV level, as is the case in our empirical example. Furthermore, graphical plots such as the right panel of Figure 8 provide intuitive guidance for model modification.

In the MV-level fit assessment, our method helps to identify curvilinear relationships in the mean and/or variance functions. In the case of item 7 in our empirical example, the misfitting linear normal factor model tended to overestimate the conditional mean of log-RT while underestimating the conditional variance at the high end of the LV. Such misfits can be particularly problematic if researchers' focus is on investigating extremely slow responders. Similar discussions can also be found in Liu and Wang (2022), where similar patterns of curvatures in the conditional moment functions have been identified using a semiparametric approach.

Several avenues for future research can be explored based on the current work.

First, beyond the example test statistics provided, other statistics can be constructed under our framework to evaluate different types of model assumptions. One simple application is to formulate generalized residuals regarding the conditional covariance between two MVs, which can yield GOF test statistic for assessing the pairwise local independence assumption (e.g., Ip, 2001; McDonald, 1994; Strout, 1990).

Second, although we focused only the common factor model in this paper, the theory we present can be extended to other measurement models, as long as a fully specified parametric model is assumed. For example, the framework can be generalized to GOF assessments in non-linear factor analysis (e.g., Yalcin and Amemiya, 2001) and count data IRT (e.g., Wang, 2010).

Finally, exploring efficient ways to compute and visualize generalized residuals when dealing with high-dimensional LVs is a potential topic for future research. When the latent dimensionality is high, it is impossible to construct evaluation points using an outer product grid as the number of evaluation points grows exponentially fast. For example, in a five-dimensional case, examining residuals at just five different points per LV leads to $5^5 = 3,125$ evaluations, making it computationally intensive and posing a challenge for generating graphical plots. Additionally, selecting which grids of LVs to summarize the results would also be challenging. Formulating partially marginalized residuals conditioned only on one or two LV(s) may yield more informative diagnostics.

References

- Alexander, P. A., Dumas, D., Grossnickle, E. M., List, A., & Firetto, C. M. (2016). Measuring relational reasoning. *The Journal of Experimental Education*, 84(1), 119–151.
- Bentler, P. M. (1990). Comparative fit indexes in structural models. *Psychological bulletin*, 107(2), 238.
- Bentler, P. M. (1995). *Eqs structural equations program manual* (Vol. 6). Multivariate software Encino, CA.
- Bickel, P. J., & Doksum, K. A. (2015). *Mathematical statistics: Basic ideas and selected topics, volume i*. Chapman; Hall/CRC.
- Bollen, K. A. (1989). *Structural equations with latent variables* (Vol. 210). John Wiley & Sons.
- Box, G. E. (1954). Some theorems on quadratic forms applied in the study of analysis of variance problems, i. effect of inequality of variance in the one-way classification. *The annals of mathematical statistics*, 290–302.
- Eid, M., Krumm, S., Koch, T., & Schulze, J. (2018). Bifactor models for predicting criteria by general and specific factors: Problems of nonidentifiability and alternative solutions. *Journal of Intelligence*, 6(3), 42.
- Haberman, S. J., Liu, Y., & Lee, Y.-H. (2019). Distractor analysis for multiple-choice tests: An empirical study with international language assessment data. *ETS Research Report Series*, 2019(1), 1–16.
- Haberman, S. J., & Sinharay, S. (2013). Generalized residuals for general models for contingency tables with application to item response theory. *Journal of the American Statistical Association*, 108(504), 1435–1444.
- Haberman, S. J., Sinharay, S., & Chon, K. H. (2013). Assessing item fit for unidimensional item response theory models using residuals from estimated item response functions. *Psychometrika*, 78, 417–440.
- Holzinger, K. J., & Swineford, F. (1937). The bi-factor method. *Psychometrika*, 2(1), 41–54.
- Hu, L.-t., & Bentler, P. M. (1999). Cutoff criteria for fit indexes in covariance structure analysis: Conventional criteria versus new alternatives. *Structural equation modeling: a multidisciplinary journal*, 6(1), 1–55.
- Imhof, J.-P. (1961). Computing the distribution of quadratic forms in normal variables. *Biometrika*, 48(3/4), 419–426.
- Ip, E. H.-s. (2001). Testing for local dependency in dichotomous and polytomous item response models. *Psychometrika*, 66(1), 109–132.

- Jöreskog, K. G. (1969). A general approach to confirmatory maximum likelihood factor analysis. *Psychometrika*, 34(2), 183–202.
- Kaplan, D. (2008). *Structural equation modeling: Foundations and extensions* (Vol. 10). SAGE publications.
- Kline, R. B. (2023). *Principles and practice of structural equation modeling*. Guilford publications.
- Lawley, D. N., & Maxwell, A. E. (1971). *Factor analysis as a statistical method*. London: Butterworth.
- Liu, Y., & Maydeu-Olivares, A. (2014). Identifying the source of misfit in item response theory models. *Multivariate Behavioral Research*, 49(4), 354–371.
- Liu, Y., & Wang, W. (2022). Semiparametric factor analysis for item-level response time data. *psychometrika*, 87(2), 666–692.
- Liu, Y., Yang, J. S., & Maydeu-Olivares, A. (2019). Restricted recalibration of item response theory models. *psychometrika*, 84, 529–553.
- Magnus, J. R., & Neudecker, H. (1999). *Matrix differential calculus with applications in statistics and econometrics*. New York: Wiley.
- Mardia, K. V. (1970). Measures of multivariate skewness and kurtosis with applications. *Biometrika*, 57(3), 519–530.
- Mardia, K. V. (1980). 9 tests of univariate and multivariate normality. *Handbook of statistics*, 1, 279–320.
- Maydeu-Olivares, A., & Joe, H. (2008). An overview of limited information goodness-of-fit testing in multidimensional contingency tables. *New trends in psychometrics*, 253–262.
- McDonald, R. P. (1994). Testing for approximate dimensionality. *Modern theories of measurement: Problems and issues*, 31–61.
- McDonald, R. P. (1999). *Test theory : A unified treatment*. Mahwah (N.J.) : Erlbaum.
- Monroe, S. (2021). Testing latent variable distribution fit in irt using posterior residuals. *Journal of Educational and Behavioral Statistics*, 46(3), 374–398.
- R Core Team. (2024). *R: A language and environment for statistical computing*. R Foundation for Statistical Computing. Vienna, Austria. <https://www.R-project.org/>
- Reiser, M. (1996). Analysis of residuals for the multinomial item response model. *Psychometrika*, 61, 509–528.
- Rosseel, Y. (2012). lavaan: An R package for structural equation modeling. *Journal of Statistical Software*, 48(2), 1–36. <https://doi.org/10.18637/jss.v048.i02>
- Satorra, A., & Bentler, P. M. (1994). Corrections to test statistics and standard errors in covariance structure analysis.

- Satterthwaite, F. E. (1946). An approximate distribution of estimates of variance components. *Biometrics bulletin*, 2(6), 110–114.
- Schott, J. R. (2016). *Matrix analysis for statistics*. John Wiley & Sons.
- Steiger, J. H., & Lind, J. C. (1980). Statistically based tests for the number of common factors. *Paper presented at the Annual Meeting of the Psychometric Society, Iowa City, 1980*.
- Strout, W. F. (1990). A new item response theory modeling approach with applications to unidimensionality assessment and ability estimation. *Psychometrika*, 55(2), 293–325.
- Tucker, L. R., & Lewis, C. (1973). A reliability coefficient for maximum likelihood factor analysis. *Psychometrika*, 38(1), 1–10.
- van der Linden, W. J. (2006). A lognormal model for response times on test items. *Journal of Educational and Behavioral Statistics*, 31(2), 181–204.
- van Rijn, P. W., Sinharay, S., Haberman, S. J., & Johnson, M. S. (2016). Assessment of fit of item response theory models used in large-scale educational survey assessments. *Large-Scale Assessments in Education*, 4, 1–23.
- Wang, L. (2010). Irt–zip modeling for multivariate zero-inflated count data. *Journal of Educational and Behavioral Statistics*, 35(6), 671–692.
- Yalcin, I., & Amemiya, Y. (2001). Nonlinear factor analysis as a statistical method. *Statistical science*, 275–294.
- Zhao, H., Alexander, P. A., & Sun, Y. (2021). Relational reasoning’s contributions to mathematical thinking and performance in chinese elementary and middle-school students. *Journal of Educational Psychology*, 113(2), 279.

Supplementary Document for
“A New Fit Assessment Framework for Common Factor Models Using Generalized Residuals”

A. Asymptotic Normality of Residuals

A.1. Assumptions

The following assumptions are made for the latent variable measurement model (with likelihood function expressed by Equation 2). Throughout Appendix A, we assume that $\mathbf{X} \in \mathcal{R}^{k \times d}$ is fixed.

(A1) *The maximum likelihood (ML) estimator (i.e., Equation 23) is \sqrt{n} -consistent. In particular,*

$$\sqrt{n}(\hat{\boldsymbol{\xi}} - \boldsymbol{\xi}) = \boldsymbol{\mathcal{I}}^{-1}(\boldsymbol{\xi}) \frac{1}{\sqrt{n}} \sum_{i=1}^n \nabla_{\boldsymbol{\xi}} \log f(\mathbf{Y}_i; \boldsymbol{\xi})^\top + o_p(1), \quad (\text{S1})$$

in which the information matrix $\boldsymbol{\mathcal{I}}(\boldsymbol{\xi}) = \mathbb{E}[\nabla_{\boldsymbol{\xi}} \log f(\mathbf{Y}_i; \boldsymbol{\xi})^\top \nabla_{\boldsymbol{\xi}} \log f(\mathbf{Y}_i; \boldsymbol{\xi})] = -\mathbb{E}[\nabla_{\boldsymbol{\xi}\boldsymbol{\xi}}^2 \log f(\mathbf{Y}_i; \boldsymbol{\xi})]$ is positive definite, and $\nabla_{\boldsymbol{\xi}\boldsymbol{\xi}}^2 \log f$ denotes the $q \times q$ Hessian matrix of the log-likelihood.

(A2) *There exists an $\omega > 0$ and the associated $\mathcal{F}_\omega = \{\boldsymbol{\xi}_1 : \|\boldsymbol{\xi}_1 - \boldsymbol{\xi}\| \leq \omega\}$ such that for all $\mathbf{y} \in \mathcal{R}^m$ and $\boldsymbol{\xi}_1, \boldsymbol{\xi}_2 \in \mathcal{F}_\omega$,*

$$\|\mathbf{H}(\mathbf{X}, \mathbf{y}, \boldsymbol{\xi}_1) - \mathbf{H}(\mathbf{X}, \mathbf{y}, \boldsymbol{\xi}_2)\| \leq b(\mathbf{y}) \|\boldsymbol{\xi}_1 - \boldsymbol{\xi}_2\|, \quad (\text{S2})$$

in which $\|\cdot\|$ denotes the ℓ_2 -norm of a vector. Furthermore, the function $b(\mathbf{y})$ in Equation S2 is squared integrable, i.e., $\int b(\mathbf{y})^2 f(\mathbf{y}, \boldsymbol{\xi}) d\mathbf{y} < \infty$.

(A3) *As $\omega \downarrow 0$,*

$$\sup_{\boldsymbol{\xi}_1 \in \mathcal{F}_\omega} \left\| \int \mathbf{H}(\mathbf{X}, \mathbf{y}, \boldsymbol{\xi}_1) \left[f(\mathbf{y}; \boldsymbol{\xi}_1) - f(\mathbf{y}; \boldsymbol{\xi}) - \nabla_{\boldsymbol{\xi}} \log f(\mathbf{y}; \boldsymbol{\xi})(\boldsymbol{\xi}_1 - \boldsymbol{\xi}) f(\mathbf{y}, \boldsymbol{\xi}) \right] d\mathbf{y} \right\| = o(\omega). \quad (\text{S3})$$

A.2. Proof

Let $\mathbb{P}_n = n^{-1} \sum_{i=1}^n \delta_{\mathbf{y}_i}$ denotes the empirical measure where $\delta_{\mathbf{y}_i}$ denotes a Dirac measure concentrating on \mathbf{y}_i . By the definitions of $\hat{\boldsymbol{\eta}}$ and $\boldsymbol{\eta}$ (Equations 25 and 26), we

rewrite the left-hand side of Equation 28 as

$$\begin{aligned}
& \sqrt{n} \left[\hat{\boldsymbol{\eta}}(\mathbf{X}, \hat{\boldsymbol{\xi}}) - \boldsymbol{\eta}(\mathbf{X}, \hat{\boldsymbol{\xi}}) \right] = \sqrt{n} \left\{ \int \mathbf{H}(\mathbf{X}, \mathbf{y}, \hat{\boldsymbol{\xi}}) \mathbb{P}_n(d\mathbf{y}) - \int \mathbf{H}(\mathbf{X}, \mathbf{y}, \hat{\boldsymbol{\xi}}) f(\mathbf{y}; \hat{\boldsymbol{\xi}}) d\mathbf{y} \right\} \\
& = \underbrace{\sqrt{n} \left\{ \int \left[\mathbf{H}(\mathbf{X}, \mathbf{y}, \hat{\boldsymbol{\xi}}) - \mathbf{H}(\mathbf{X}, \mathbf{y}, \boldsymbol{\xi}) \right] [\mathbb{P}_n(d\mathbf{y}) - f(\mathbf{y}; \boldsymbol{\xi}) d\mathbf{y}] \right\}}_{\text{(I)}} \\
& \quad - \underbrace{\sqrt{n} \int \mathbf{H}(\mathbf{X}, \mathbf{y}, \hat{\boldsymbol{\xi}}) \left[f(\mathbf{y}; \hat{\boldsymbol{\xi}}) - f(\mathbf{y}; \boldsymbol{\xi}) \right] d\mathbf{y}}_{\text{(II)}} \\
& \quad + \underbrace{\sqrt{n} \int \mathbf{H}(\mathbf{X}, \mathbf{y}, \boldsymbol{\xi}) [\mathbb{P}_n(d\mathbf{y}) - f(\mathbf{y}; \boldsymbol{\xi}) d\mathbf{y}]}_{\text{(III)}}. \tag{S4}
\end{aligned}$$

It suffices to show that

$$\text{(I)} = o_p(1), \tag{S5}$$

and that

$$\text{(II)} = \mathbf{A}(\mathbf{X}, \boldsymbol{\xi}) \mathcal{I}^{-1}(\boldsymbol{\xi}) \frac{1}{\sqrt{n}} \sum_{i=1}^n \nabla_{\boldsymbol{\xi}} \log f(\mathbf{Y}_i; \boldsymbol{\xi})^\top + o_p(1), \tag{S6}$$

in which $\mathbf{A}(\mathbf{X}, \boldsymbol{\xi}) = \mathbb{E} [\mathbf{H}(\mathbf{X}, \mathbf{Y}_i, \boldsymbol{\xi}) \nabla_{\boldsymbol{\xi}} \log f(\mathbf{Y}_i; \boldsymbol{\xi})] = \text{Cov} [\mathbf{H}(\mathbf{X}, \mathbf{Y}_i, \boldsymbol{\xi}), \nabla_{\boldsymbol{\xi}} \log f(\mathbf{Y}_i; \boldsymbol{\xi})]$. Note that $\mathbf{A}(\mathbf{X}, \boldsymbol{\xi})$ is finite because both $\nabla_{\boldsymbol{\xi}} \log f$ and \mathbf{H} are squared integrable in the light of Assumptions (A1) and (A2). Further let $\boldsymbol{\Sigma}_{\mathbf{H}}(\mathbf{X}, \boldsymbol{\xi}) = \text{Cov}[\mathbf{H}(\mathbf{X}, \mathbf{Y}_i, \boldsymbol{\xi})]$ and denote column-wise concatenation of matrix blocks by a colon (:). As a consequence of Slutsky's Theorem and the Central Limit Theorem,

$$\begin{aligned}
& \sqrt{n} \left[\hat{\boldsymbol{\eta}}(\mathbf{X}, \hat{\boldsymbol{\xi}}) - \boldsymbol{\eta}(\mathbf{X}, \hat{\boldsymbol{\xi}}) \right] \\
& = \left[-\mathbf{A}(\mathbf{X}, \boldsymbol{\xi}) \mathcal{I}^{-1}(\boldsymbol{\xi}) : \mathbf{I}_{k \times k} \right] \sqrt{n} \begin{bmatrix} n^{-1} \sum_{i=1}^n \nabla_{\boldsymbol{\xi}} \log f(\mathbf{Y}_i; \boldsymbol{\xi})^\top \\ n^{-1} \sum_{i=1}^n \mathbf{H}(\mathbf{X}, \mathbf{Y}_i, \boldsymbol{\xi}) - \boldsymbol{\eta}(\mathbf{X}, \boldsymbol{\xi}) \end{bmatrix} + o_p(1) \\
& \xrightarrow{d} \mathcal{N}(\mathbf{0}, -\mathbf{A}(\mathbf{X}, \boldsymbol{\xi}) \mathcal{I}^{-1}(\boldsymbol{\xi}) \mathbf{A}(\mathbf{X}, \boldsymbol{\xi})^\top + \boldsymbol{\Sigma}_{\mathbf{H}}(\mathbf{X}, \boldsymbol{\xi})), \tag{S7}
\end{aligned}$$

which is the desired result (i.e., the right-hand side of Equation 28).

To establish Equation S5, we note that $\sqrt{n}[\mathbb{P}_n(d\mathbf{y}) - f(\mathbf{y}; \boldsymbol{\xi})d\mathbf{y}]$ is the empirical process (van der Vaart, 2000, Chapter 19), and that $\mathbf{H}(\mathbf{X}, \cdot, \hat{\boldsymbol{\xi}})$ can be viewed as a random function (of \mathbf{y}) that estimates $\mathbf{H}(\mathbf{X}, \cdot, \boldsymbol{\xi})$ (as $\hat{\boldsymbol{\xi}} \xrightarrow{p} \boldsymbol{\xi}$ when the model is correctly specified). Then Equation S5 is a straightforward consequence of Lemma 19.24 in van der Vaart (2000) provided (a) $\{\mathbf{H}(\mathbf{X}, \cdot, \boldsymbol{\xi}_1) : \boldsymbol{\xi}_1 \in \mathcal{F}_\omega\}$ is a Donsker class and (b) $\int \left\| \mathbf{H}(\mathbf{X}, \mathbf{y}, \hat{\boldsymbol{\xi}}) - \mathbf{H}(\mathbf{X}, \mathbf{y}, \boldsymbol{\xi}) \right\|^2 f(\mathbf{y}; \boldsymbol{\xi}) d\mathbf{y} \xrightarrow{p} 0$ under the correctly specified model. Both (a) and (b) are guaranteed by Assumption (A2); see Example 19.7 of van der Vaart (2000). To

show Equation S6, note that (II) can be further bounded by

$$\begin{aligned}
(\text{II}) &= \underbrace{\sqrt{n} \int \mathbf{H}(\mathbf{X}, \mathbf{y}, \hat{\boldsymbol{\xi}}) \left[f(\mathbf{y}; \hat{\boldsymbol{\xi}}) - f(\mathbf{y}; \boldsymbol{\xi}) - \nabla_{\boldsymbol{\xi}} \log f(\mathbf{y}; \boldsymbol{\xi})(\hat{\boldsymbol{\xi}} - \boldsymbol{\xi}) f(\mathbf{y}, \boldsymbol{\xi}) \right] d\mathbf{y}}_{(\text{II.a})} \\
&\quad + \underbrace{\sqrt{n} \int [\mathbf{H}(\mathbf{X}, \mathbf{y}, \hat{\boldsymbol{\xi}}) - \mathbf{H}(\mathbf{X}, \mathbf{y}, \boldsymbol{\xi})] \nabla_{\boldsymbol{\xi}} \log f(\mathbf{y}; \boldsymbol{\xi})(\hat{\boldsymbol{\xi}} - \boldsymbol{\xi}) f(\mathbf{y}, \boldsymbol{\xi}) d\mathbf{y}}_{(\text{II.b})} \\
&\quad + \underbrace{\sqrt{n} \int \mathbf{H}(\mathbf{X}, \mathbf{y}, \boldsymbol{\xi}) \nabla_{\boldsymbol{\xi}} \log f(\mathbf{y}; \boldsymbol{\xi})(\hat{\boldsymbol{\xi}} - \boldsymbol{\xi}) f(\mathbf{y}, \boldsymbol{\xi}) d\mathbf{y}}_{(\text{II.c})}. \tag{S8}
\end{aligned}$$

In Equation S8, (II.a) = $o_p(1)$ is a direct consequence of Assumption (A3) and the \sqrt{n} -consistency of $\hat{\boldsymbol{\xi}}$. Moreover,

$$\|(\text{II.b})\| \lesssim \sqrt{n} \|\hat{\boldsymbol{\xi}} - \boldsymbol{\xi}\|^2 \left[\int b(\mathbf{y})^2 f(\mathbf{y}; \boldsymbol{\xi}) d\mathbf{y} \right]^{1/2} \left[\int \|\nabla_{\boldsymbol{\xi}} \log f(\mathbf{y}; \boldsymbol{\xi})\|^2 f(\mathbf{y}; \boldsymbol{\xi}) d\mathbf{y} \right]^{1/2}, \tag{S9}$$

by the Cauchy-Schwarz inequality, in which $x \lesssim y$ means $x \leq Cy$ for some constant C . The squared integrability of $b(\mathbf{y})$ and $\nabla_{\boldsymbol{\xi}} \log f(\mathbf{y}; \boldsymbol{\xi})$ guarantees that the right-hand side of Equation S9 is also $o_p(1)$. Finally, the definition of $\mathbf{A}(\mathbf{X}, \boldsymbol{\xi})$ and Assumption (A1) imply that (II.c) = $\mathbf{A}(\mathbf{X}, \boldsymbol{\xi}) \boldsymbol{\mathcal{I}}^{-1}(\boldsymbol{\xi}) n^{-1/2} \sum_{i=1}^n \nabla_{\boldsymbol{\xi}} \log f(\mathbf{Y}_i; \boldsymbol{\xi})^\top + o_p(1)$. The proof is now complete.

A.3. Common Factor Models

We proceed to check Assumptions (A1)–(A3) for the common factor model.

Assumption (A1) is implied by standard regularity conditions for the ML estimator, which can be found in many statistical textbooks (e.g., Bickel and Doksum, 2015, Chapter 6; van der Vaart, 2000, Chapter 5). Specifically for mean and covariance structure models of multivariate normal data, which subsumes the common factor model as a special case, readers may refer to, for example, Shapiro (2007) and Chapter 15 of Magnus and Neudecker (2019).

Assumption (A2) requires that the function \mathbf{H} is locally Lipschitz continuous in $\boldsymbol{\xi}$ with a squared integrable Lipschitz constant $b(\mathbf{y})$ (with respect to $f(\mathbf{y}; \boldsymbol{\xi}) d\mathbf{y}$). Under a common factor model, each component of \mathbf{H} , which has been expressed in Equation 10 as $H(\mathbf{x}, \mathbf{y}, \boldsymbol{\xi})$, is in fact continuously differentiable in $\boldsymbol{\xi}$. Hence, we only need to verify that the derivatives of H for all $\boldsymbol{\xi}$ in some \mathcal{F}_ω are uniformly dominated by an integrable function. To this end, note that

$$\nabla_{\boldsymbol{\xi}} H(\mathbf{x}, \mathbf{y}, \boldsymbol{\xi}) = \frac{f(\mathbf{y}|\mathbf{x})}{f(\mathbf{y})} [\nabla_{\boldsymbol{\xi}} h(\mathbf{x}, \mathbf{y}, \boldsymbol{\xi}) + \nabla_{\boldsymbol{\xi}} \log f(\mathbf{y}|\mathbf{x}) - \nabla_{\boldsymbol{\xi}} \log f(\mathbf{y})]. \tag{S10}$$

Because both $f(\mathbf{y}|\mathbf{x})$ and $f(\mathbf{y})$ are densities of multivariate normal distributions (and therefore bounded and log-quadratic in \mathbf{y} ; see Equations 5 and 6) and our choices of h 's are at most quadratic in \mathbf{y} , we have

$$|\nabla_{\boldsymbol{\xi}} H(\mathbf{x}, \mathbf{y}, \boldsymbol{\xi})| \leq |a_0(\mathbf{x}, \boldsymbol{\xi}) + \mathbf{a}_1(\mathbf{x}, \boldsymbol{\xi})^\top \mathbf{y} + \mathbf{y}^\top \mathbf{A}_2(\mathbf{x}, \boldsymbol{\xi}) \mathbf{y}|, \quad (\text{S11})$$

in which the coefficients of the quadratic function, denoted by $a_0(\mathbf{x}, \boldsymbol{\xi}) \in \mathcal{R}$, $\mathbf{a}_1(\mathbf{x}, \boldsymbol{\xi}) \in \mathcal{R}^m$, and $\mathbf{A}_2(\mathbf{x}, \boldsymbol{\xi}) \in \mathcal{R}^{m \times m}$, are all continuous in $\boldsymbol{\xi}$. Together with the fact that polynomial functions are integrable under multivariate normal distributions, there exists some $\omega > 0$ such that the right-hand side of Equation S11 for all $\boldsymbol{\xi} \in \mathcal{F}_\omega$ can be uniformly dominated, which establishes Assumption (A2).

Assumption (A3) is closely related to the Fréchet differentiability of a probability measure. To verify Assumption (A3), we first obtain the Taylor-series expansion of $f(\mathbf{y}; \boldsymbol{\xi}_1)$, where $\boldsymbol{\xi}_1 \in \mathcal{F}_\omega$, at $\boldsymbol{\xi}$:

$$\begin{aligned} f(\mathbf{y}; \boldsymbol{\xi}_1) &= f(\mathbf{y}; \boldsymbol{\xi}) + f(\mathbf{y}; \boldsymbol{\xi}) \nabla_{\boldsymbol{\xi}} \log f(\mathbf{y}; \boldsymbol{\xi}) (\boldsymbol{\xi}_1 - \boldsymbol{\xi}) \\ &\quad + \frac{f(\mathbf{y}; \boldsymbol{\zeta})}{2} (\boldsymbol{\xi}_1 - \boldsymbol{\xi})^\top [\nabla_{\boldsymbol{\xi}\boldsymbol{\xi}}^2 \log f(\mathbf{y}; \boldsymbol{\zeta}) + \nabla_{\boldsymbol{\xi}} \log f(\mathbf{y}; \boldsymbol{\zeta})^\top \nabla_{\boldsymbol{\xi}} \log f(\mathbf{y}; \boldsymbol{\zeta})] (\boldsymbol{\xi}_1 - \boldsymbol{\xi}), \end{aligned} \quad (\text{S12})$$

in which $\boldsymbol{\zeta} = \gamma \boldsymbol{\xi}_1 + (1 - \gamma) \boldsymbol{\xi}$ for some $\gamma \in [0, 1]$. Then we have

$$\begin{aligned} &\left\| \int \mathbf{H}(\mathbf{X}, \mathbf{y}, \boldsymbol{\xi}_1) \left[f(\mathbf{y}; \boldsymbol{\xi}_1) - f(\mathbf{y}; \boldsymbol{\xi}) - \nabla_{\boldsymbol{\xi}} \log f(\mathbf{y}; \boldsymbol{\xi}) (\boldsymbol{\xi}_1 - \boldsymbol{\xi}) f(\mathbf{y}, \boldsymbol{\xi}) \right] d\mathbf{y} \right\| \\ &\lesssim \frac{1}{2} (\boldsymbol{\xi}_1 - \boldsymbol{\xi})^\top \left\{ \int \|\mathbf{H}(\mathbf{X}, \mathbf{y}, \boldsymbol{\xi})\| \left[\nabla_{\boldsymbol{\xi}\boldsymbol{\xi}}^2 \log f(\mathbf{y}; \boldsymbol{\zeta}) \right. \right. \\ &\quad \left. \left. + \nabla_{\boldsymbol{\xi}} \log f(\mathbf{y}; \boldsymbol{\zeta})^\top \nabla_{\boldsymbol{\xi}} \log f(\mathbf{y}; \boldsymbol{\zeta}) \right] f(\mathbf{y}; \boldsymbol{\zeta}) d\mathbf{y} \right\} (\boldsymbol{\xi}_1 - \boldsymbol{\xi}). \end{aligned} \quad (\text{S13})$$

The first and second derivatives of the multivariate normal log-likelihood are quadratic in \mathbf{y} (e.g., Magnus and Neudecker, 2019, Section 15.3). From our earlier argument to verify Assumption (A2), we also know that the components of \mathbf{H} considered in the current work are at most quadratic in \mathbf{y} . Therefore, the integral on the right-hand side of Equation S13 is uniformly bounded for all $\boldsymbol{\zeta} \in \mathcal{F}_\omega$, which further implies that Equation S13 is $o(\omega)$.

B. Transformed Residuals

Let $\varphi : \mathcal{R}^k \rightarrow \mathcal{R}^{k'}$, $k' < k$, be a twice continuously differentiable transformation and $\nabla\varphi$ be the corresponding $k' \times k$ Jacobian matrix. To establish asymptotic normality for the transformed residuals (Equation 30), we Taylor-expand $\varphi(\hat{\boldsymbol{\eta}}(\mathbf{X}, \hat{\boldsymbol{\xi}}))$ at $\boldsymbol{\eta}(\mathbf{X}, \hat{\boldsymbol{\xi}})$ and obtain

$$\begin{aligned}\sqrt{n}\mathbf{e}_\varphi(\mathbf{X}) &= \sqrt{n} \left[\varphi(\hat{\boldsymbol{\eta}}(\mathbf{X}, \hat{\boldsymbol{\xi}})) - \varphi(\boldsymbol{\eta}(\mathbf{X}, \hat{\boldsymbol{\xi}})) \right] \\ &= \sqrt{n} \nabla\varphi(\boldsymbol{\eta}(\mathbf{X}, \hat{\boldsymbol{\xi}})) \left[\hat{\boldsymbol{\eta}}(\mathbf{X}, \hat{\boldsymbol{\xi}}) - \boldsymbol{\eta}(\mathbf{X}, \hat{\boldsymbol{\xi}}) \right] + \mathbf{R}_n.\end{aligned}\quad (\text{S14})$$

The remainder vector \mathbf{R}_n can be explicitly expressed as

$$\mathbf{R}_n = \begin{bmatrix} R_{n,1} \\ \vdots \\ R_{n,k'} \end{bmatrix} = \frac{1}{2} \begin{bmatrix} \sqrt{n} \left(\hat{\boldsymbol{\eta}}(\mathbf{X}, \hat{\boldsymbol{\xi}}) - \boldsymbol{\eta}(\mathbf{X}, \hat{\boldsymbol{\xi}}) \right)^\top \nabla^2\varphi_{1.}(\boldsymbol{\zeta}_n) \left(\hat{\boldsymbol{\eta}}(\mathbf{X}, \hat{\boldsymbol{\xi}}) - \boldsymbol{\eta}(\mathbf{X}, \hat{\boldsymbol{\xi}}) \right) \\ \vdots \\ \sqrt{n} \left(\hat{\boldsymbol{\eta}}(\mathbf{X}, \hat{\boldsymbol{\xi}}) - \boldsymbol{\eta}(\mathbf{X}, \hat{\boldsymbol{\xi}}) \right)^\top \nabla^2\varphi_{k'.}(\boldsymbol{\zeta}_n) \left(\hat{\boldsymbol{\eta}}(\mathbf{X}, \hat{\boldsymbol{\xi}}) - \boldsymbol{\eta}(\mathbf{X}, \hat{\boldsymbol{\xi}}) \right) \end{bmatrix}. \quad (\text{S15})$$

In Equation S15, $\nabla^2\varphi_{i.}$, $i = 1, \dots, k'$, denotes the $k \times k$ Jacobian of $\nabla\varphi_{i.}$, which is the transpose of the i th row of $\nabla\varphi$ (i.e., a $k \times 1$ column vector), and $\boldsymbol{\zeta}_n = \gamma\hat{\boldsymbol{\eta}}(\mathbf{X}, \hat{\boldsymbol{\xi}}) + (1 - \gamma)\boldsymbol{\eta}(\mathbf{X}, \hat{\boldsymbol{\xi}})$ with some $\gamma \in [0, 1]$. Each component of \mathbf{R}_n , i.e., $R_{n,i}$, is $o_p(1)$ because $\sqrt{n}[\hat{\boldsymbol{\eta}}(\mathbf{X}, \hat{\boldsymbol{\xi}}) - \boldsymbol{\eta}(\mathbf{X}, \hat{\boldsymbol{\xi}})] = O_p(1)$ (Equation S7) and $\nabla^2\varphi_{i.}(\boldsymbol{\zeta}_n) \xrightarrow{p} \nabla^2\varphi_{i.}(\boldsymbol{\eta}(\mathbf{X}, \boldsymbol{\xi}))$. By $\nabla\varphi(\boldsymbol{\eta}(\mathbf{X}, \hat{\boldsymbol{\xi}})) \xrightarrow{p} \nabla\varphi(\boldsymbol{\eta}(\mathbf{X}, \boldsymbol{\xi}))$ and Slutsky's Theorem, Equation S14 implies that

$$\sqrt{n}\mathbf{e}_\varphi(\mathbf{X}) \xrightarrow{d} \mathcal{N}(\mathbf{0}, \boldsymbol{\Sigma}_\varphi(\mathbf{X}, \boldsymbol{\xi})), \quad (\text{S16})$$

in which $\boldsymbol{\Sigma}_\varphi(\mathbf{X}, \boldsymbol{\xi}) = \nabla\varphi(\boldsymbol{\eta}(\mathbf{X}, \boldsymbol{\xi})) \left[-\mathbf{A}(\mathbf{X}, \boldsymbol{\xi})\mathcal{I}^{-1}(\boldsymbol{\xi})\mathbf{A}(\mathbf{X}, \boldsymbol{\xi})^\top + \boldsymbol{\Sigma}_\mathbf{H}(\mathbf{X}, \boldsymbol{\xi}) \right] \nabla\varphi(\boldsymbol{\eta}(\mathbf{X}, \boldsymbol{\xi}))^\top$ (i.e., Equation 31).

C. Empirical Data Analysis Using the Simple Estimator

Using the empirical data presented in Section 4, we address the distinction between using the ratio and simple estimators for MV/item-level fit assessment. In the item fit assessment, where we consistently applied the ratio estimator in the main text, fit diagnostics are conducted (approximately) independently of the correct specification of the LV density. This is because the ratio estimator estimates the LV density within its formula, as already noted in Section 2.2.3. Although the impact of misfit in LV density cannot be completely eliminated since the estimates of LV density may not exactly reproduce the true density, we can still interpret the results in Figures 9 and 10 as fit diagnostics under the assumption of a correctly specified LV density.

In contrast, using the simple estimator for the same fit assessment would likely lead to all items displaying a similar pattern, due to the influence of a misspecified LV density. Figures S1 and S2 present the item fit assessment results using the simple estimator, where noticeably different shapes compared to the results obtained with the ratio estimator can

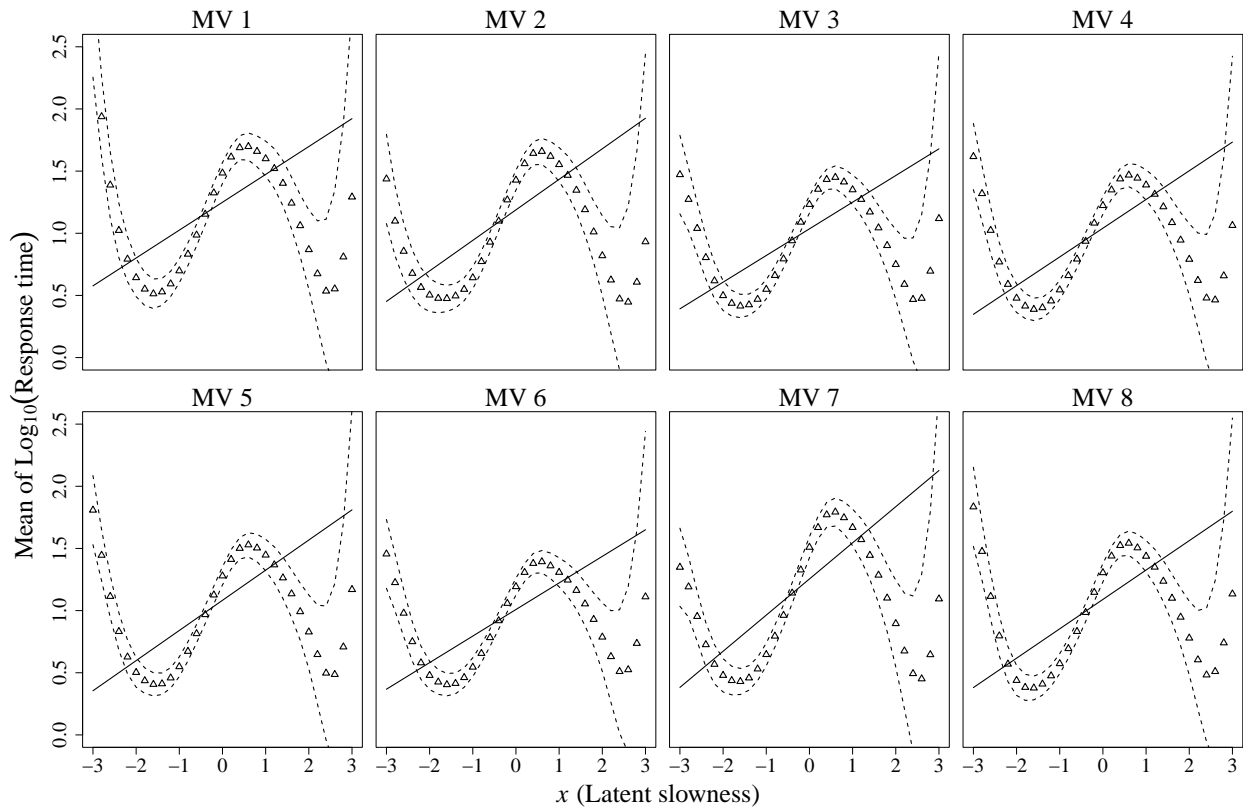
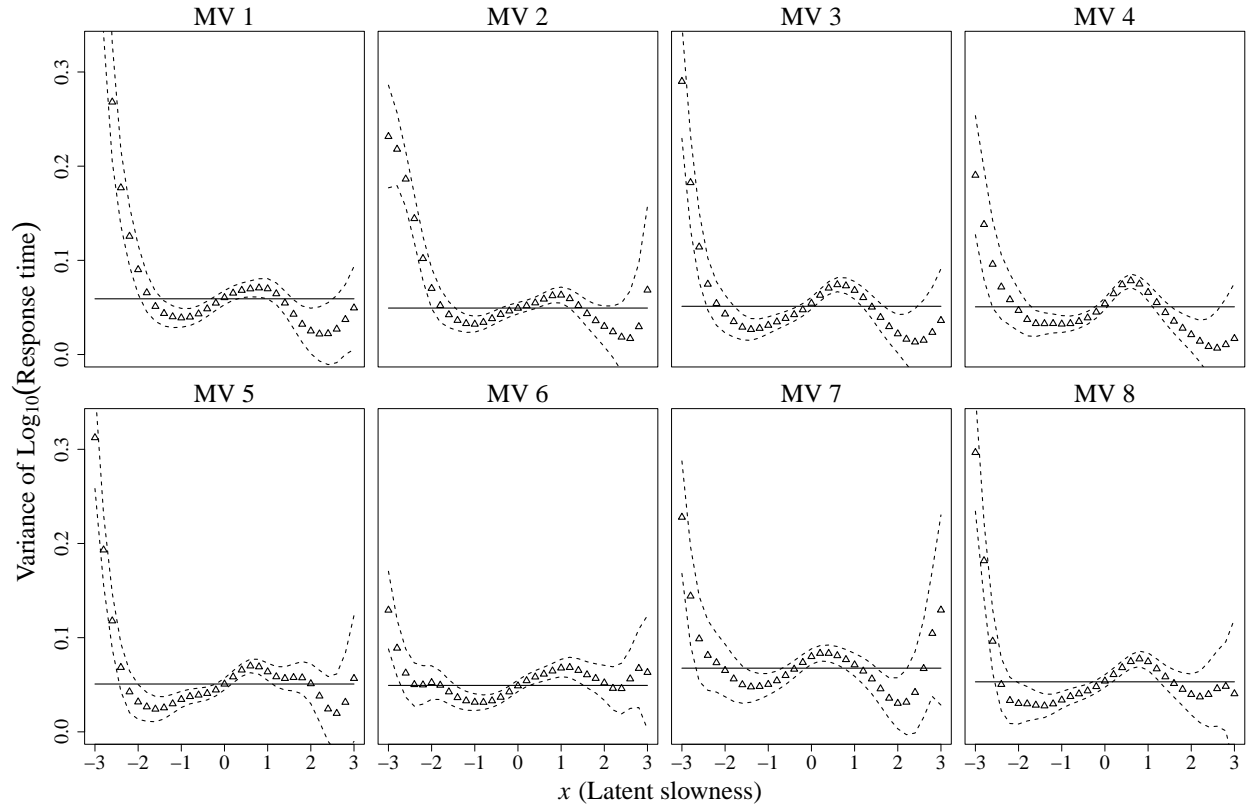


Figure S1

Conditional mean functions of the empirical example analyzed with the simple estimator. Solid lines represent model-implied linear mean functions. Triangular points are the simple estimators obtained at each point. Dashed lines delineate a 95% pointwise confidence band.

**Figure S2**

Conditional variance functions of the empirical example analyzed with the simple estimator. Solid lines represent model-implied constant variance functions. Triangular points are the simple estimators obtained at each point. Dashed lines delineate a 95% pointwise confidence band.

be observed: the conditional mean and variance functions show a consistent pattern across all items. Although this similar pattern across all items also provides diagnostic information on badness of fit, this result may not be optimal for the purpose of item-level fit assessment, as it fails to differentiate between well-fitting and poorly-fitting items.

References

- Bickel, P., & Doksum, K. (2015). *Mathematical statistics: Basic ideas and selected topics* (2nd ed.). CRC Press.
- Magnus, J., & Neudecker, H. (2019). *Matrix differential calculus with applications in statistics and econometrics*. Wiley.
<https://books.google.com/books?id=8DmNDwAAQBAJ>
- Shapiro, A. (2007). Statistical inference of moment structures. In S.-Y. Lee (Ed.), *Handbook of latent variable and related models* (pp. 229–260). Elsevier.
- van der Vaart, A. (2000). *Asymptotic statistics*. Cambridge University Press.